

Loco-Manipulation with Non-impulsive Contact-Implicit Planning in a Slithering Robot

A Thesis Presented

by

Kruthika Gangaraju

to

The Department of Electrical and Computer Engineering

in partial fulfillment of the requirements

for the degree of

Master of Science

in

Robotics - Concentration in Mechanical

Northeastern University

Boston, Massachusetts

April 2024

To Mom, Dad and Tanmay.

Contents

List of Figures	iv
List of Acronyms	vi
Acknowledgments	vii
Abstract of the Thesis	viii
1 Introduction	1
1.0.1 Challenges of Object Manipulation	2
1.1 Loco-manipulation	3
1.1.1 Challenges in locomanipulation	7
1.2 Classification of Loco-Manipulation Approaches	8
1.2.1 Robot Arm Manipulators	8
1.2.2 Wheeled Mobile Manipulators	9
1.2.3 Legged Mobile Manipulators	9
1.2.4 Aerial Manipulators	10
1.2.5 Continuum Manipulators	11
1.3 Prior SS Lab Works	11
1.4 COBRA Design Motivation	12
1.5 Loco-manipulation using COBRA	12
1.6 Objectives and Outline of Thesis	13
1.7 Contributions	14
2 COBRA Platform	15
2.1 COBRA Hardware	15
2.2 Simulation Setup	18
2.2.1 Actuator model	19
2.2.2 Contact force model	21
2.2.3 Environment setup for Loco-manipulation	23
2.3 Open-loop CPG gaits	25
3 Contact Modelling	28

4	Results	32
5	Conclusion	44
5.1	Challenges in existing setup	45
5.2	Future Scope	45

List of Figures

1.1	Cartoon illustration of loco-manipulation problem.	2
1.2	Illustrates a hyper-redundant robot mounted on a mobile base from A. Wolf, et al., 2005 [96], in a search and rescue mission.	5
1.3	Illustrates robot in a warehouse, M. A. Khan, 2020, [34]	6
1.4	Illustrates robot navigating around space station, S. Schneider, et al., 2021, [67] . .	6
1.5	Challenges of loco - manipulation; a) shows the difficulty of navigating through clustered, narrow spaces [6]; b) shows the challenge of taking a box up a flight of stairs [32]; c) shows a wheeled manipulator trying to pick up an object during its locomotion [97].	7
1.6	Classification of object manipulation approaches in the literature	9
1.7	Illustrates Spot picking object from table [24]	10
1.8	Illustrates a drone carrying packages [50]	11
1.9	Object manipulation using COBRA	13
2.1	This image shows the overview of COBRA model with the head coordinate frame and the coordinate frames for the yawing and pitching joints which are consistent throughout the robot. It also show the naming convention used accross all the models and codes in which Jx corresponds to the joints and Ly corresponds to the link where x ranges from 1 to 11 and y ranges from 1 to 10, excluding the head and tail. . . .	16
2.2	A single COBRA module	17
2.3	(Above) Closeup view of the head with actuated fins. (Below) Expanded view of the head module.	18
2.4	(Above) Docking module on the box. (Below) Head module latched onto the docking module on the box.	19
2.5	Simscape block for actuator model	21
2.6	Simscape contact force block	23
2.7	Simscape model setup	25
2.8	Simscape environment setup for loco-manipulation problem	26
2.9	Various gaits implemented on COBRA	27
3.1	Full-dynamics model parameters in the object manipulation task considered in this paper	29

4.1	Snapshots depicting simulated forward box push utilizing various gaits executed in Matlab. The J-shape gait is an asymmetric variation of the C-gait, which allows changing the direction of movement of the box by mirroring the gait.	33
4.2	This image depicts the contact points and unilateral ground reaction forces during (A): C-shaped gaits, (B) S-Shaped Gait, (C) J-Shaped Gait, (D) Sidewinding gait, performed by the high-fidelity COBRA model simulated in the MATLAB environment. The contact forces consist of tangential forces ($f_{T,i}$) and normal forces ($f_{N,i}$). Lx here refers to Link number x on the robot, numbered from 1-10 starting from the head.	34
4.3	Depicts the torque profile for the central yawing (J6) and pitching (J5) joints for each gait. Other joints show similar profiles offset by a phase angle based on the executed gait.	35
4.4	Depicts the efficiency of each gait based on the total work done by the robot for locomotion against total work done on the box. Larger slope indicates a less efficient gait as more work is done on locomotion in return for smaller work done on the box.	36
4.5	Shows the instantaneous power consumption by the robot to execute locomotion for each of the considered gaits.	37
4.6	Depicts the total distance the robot moves the box for each gait in the same amount of time.	37
4.7	Shows the hardware implementation of the lateral rolling gaits performed in Simscape model	38
4.8	Shows comparison between simscape and real robot of robot and box for the various lateral rolling gaits on flat ground shown from top view	39
4.9	Snapshots of COBRA lifting a box and placing it on a raised platform.	40
4.10	Snapshots depict simulation of COBRA lifting a box from a raised platform, placing it on the flat ground, and translating the box to a new location through continuous body-object interactions during slithering motions.	41
4.11	Snapshots depict COBRA lifting a box from a raised platform, placing it on the flat ground, and translating the box to a new location through continuous body-object interactions during slithering motions.	41
4.12	Snapshots capture COBRA lifting a box from a raised platform, setting it down on the ground, and ascending a ramp by continually pushing the box while lateral rolling.	42
4.13	(Left) Shows the trajectory of the box while being lifted from ground and placed on a raised platform. (Right) Shows the contact forces between the robot and ground during the entire trajectory	42
4.14	(Top) Shows the box trajectory during picking from platform, placing on ground and manipulating to the top of the ramp. (Bottom) Contact forces for the robot and box during picking the box from a raised platform, placing on the ground, and manipulation using s-lateral rolling gait up a ramp.	43

List of Acronyms

DoF Degrees of Freedom.

CPG Central Pattern Generator.

ODE Ordinary Differential Equation.

IMU Inertial Measurement Unit.

Acknowledgments

This work has been supported by a lot of people in a number of different ways. I would first like to acknowledge the mentorship and guidance provided to me by my advisor Dr. Alireza Ramezani over the course of this thesis, opening up new opportunities and perspectives for research. I would also like to acknowledge my co-advisors Dr. Gunar Schirner and Dr. Rifat Sipahi for their guidance. I would like to thank my mentor, Adarsh Salagame, for his constant support and encouragement that made the completion of this thesis possible. I would also like to acknowledge the support of other Silicon Synapse lab members, Harin Nallaguntla, Aditya Bondada, Shreyansh Pitroda, Bibek Gupta, Yogi Shah, Henry Noyes, Nolan Smithwick, Alex Qui and few others who helped with simulation and experimentation. I also want to thank my friends Komal Sajwan, Jhanvi Chande, Devansh Dedhia, Dheer Kachalia, Shreya Rahate, Aditya Gosalia, Pratyush Padhi, Ronak Bhanushali and Prem Sukhadwala for their constant support and motivation, and most importantly believing in me. Finally I would like to thank my parents, without whom none of this would be possible, my family for their encouragements and especially my brother Tanmay, who has been a constant pillar of support for me.

Abstract of the Thesis

Loco-Manipulation with Non-impulsive Contact-Implicit Planning in a
Slithering Robot

by

Kruthika Gangaraju

Master of Science in Robotics - Concentration in Mechanical

Northeastern University, April 2024

Dr. Alireza Ramezani, Advisor

Dr. Gunar Schirner, Co-advisor

Dr. Rifat Sipahi, Co-advisor

Object manipulation has been extensively studied in the context of fixed base and mobile manipulators. However, the overactuated locomotion modality employed by snake robots allows for a unique blend of object manipulation through locomotion, referred to as loco-manipulation. The following work presents an optimization approach to solving the loco-manipulation problem based on non-impulsive implicit contact path planning for our snake robot COBRA. This thesis presents the mathematical framework and show high-fidelity simulation results and experiments to demonstrate the effectiveness of our approach.

Chapter 1

Introduction

Object manipulation is an overlap of mechanical design, control engineering and sensor fusion aimed at providing robots with human-like ability to interact with the world. It encompasses a broad spectrum of tasks, ranging from simple pick-and-place operations to complex manipulation and assembly processes in industrial settings, as well as more sophisticated interactions in human-robot collaboration scenarios and domestic environments. Object manipulation in robots can be achieved with the use of different types of end effectors to the manipulators to achieve desired tasks. These can be in the form of claws, suction cups, or finger-like attachments.

In addition to hardware, object manipulation in robotics relies heavily on software algorithms and control systems to plan and execute manipulation tasks effectively. Machine learning and computer vision techniques play a crucial role in enabling robots to perceive and understand the environment, recognize objects, and plan appropriate manipulation strategies [17]. One of the key challenges in robotic object manipulation is achieving robustness and adaptability across diverse environments and objects. Robots must be able to handle variations in object size, shape, weight, and texture, as well as unforeseen obstacles and disturbances in the environment. This requires the development of algorithms for adaptive grasping and manipulation, as well as robust sensing and feedback mechanisms to detect and correct errors in real-time. Object manipulation has a wide range of applications across various sectors, where the ability to grasp, move, and interact with objects is essential. Some of the sectors where object manipulation is particularly useful include:

1. **Manufacturing and Industrial Automation:** Object manipulation is fundamental in manufacturing for tasks such as assembly, pick-and-place operations, packaging, and material handling. Robots equipped with manipulation capabilities increase efficiency, consistency, and



Figure 1.1: Cartoon illustration of loco-manipulation problem.

throughput in production lines while reducing labor costs and minimizing errors [2].

2. Healthcare and Medical Robotics: Object manipulation plays a vital role in healthcare for tasks such as surgical procedures, patient care, and laboratory automation. Surgical robots assist surgeons in performing minimally invasive surgeries with greater precision and dexterity, while robotic systems handle tasks such as medication dispensing, sample handling, and sterilization [31].

1.0.1 Challenges of Object Manipulation

Object manipulation in robotics presents several challenges, stemming from the complexity of interacting with the physical world in dynamic and uncertain environments [4]. Some of the key challenges include:

1. Variability in Object Properties: Objects encountered in real-world environments exhibit variability in terms of size, shape, weight, texture, and material properties. Robots must be able to adapt their manipulation strategies to handle this variability effectively. Developing algorithms that can generalize across different object types and properties remains a significant challenge.

CHAPTER 1. INTRODUCTION

2. **Grasping and Manipulation Planning:** Planning and executing grasping and manipulation actions in real-time require solving complex optimization problems. Robots must determine suitable grasp points and orientations for objects, considering factors such as stability, accessibility, and task constraints. Developing efficient algorithms for grasp planning and manipulation sequencing remains an ongoing research area.
3. **Adaptation to Uncertainty:** Real-world environments are characterized by uncertainty, including variations in object pose, unexpected obstacles, and disturbances. Robots must be able to adapt their manipulation strategies in response to uncertainty to achieve robust and reliable performance. This may involve incorporating feedback mechanisms or employing predictive models to anticipate and mitigate uncertainty.
4. **Dexterity and Manipulation Skills:** Achieving dexterous manipulation requires precise control over the robot's end-effector, whether it's a robotic hand, gripper, or manipulator. Designing robotic hands capable of emulating human-like dexterity while ensuring mechanical robustness and efficiency remains a significant engineering challenge. Moreover, developing control algorithms that enable fine-grained manipulation and coordination of multiple degrees of freedom is non-trivial.
5. **Learning and Adaptation:** Object manipulation tasks may involve handling novel objects or operating in unfamiliar environments. Robots must be able to learn from experience and adapt their manipulation strategies over time to improve performance and adapt to new situations. Developing efficient and scalable learning algorithms that can leverage large datasets or simulation environments while ensuring safety and reliability is a significant research challenge.

1.1 Loco-manipulation

"Locomotion + manipulation" refers to the integration of both mobility and manipulation capabilities in robots. It combines the ability to move through an environment (locomotion) with the capability to interact with objects within that environment (manipulation). This integration enables robots to perform a wide range of tasks that involve both navigating through space and interacting with objects.

In many robotic systems, locomotion and manipulation are treated as separate subsystems, each with its own set of sensors, actuators, and control algorithms. Locomotion systems enable

CHAPTER 1. INTRODUCTION

robots to move from one location to another, whether it's navigating across rough terrain, climbing stairs, or traversing indoor environments. These locomotion mechanisms can range from wheeled or tracked platforms to legged robots or even flying drones.

On the other hand, manipulation systems allow robots to grasp, lift, move, and manipulate objects in their environment. This may involve using robotic arms with grippers, hands, or specialized end-effectors to interact with objects in various ways. Manipulation capabilities are essential for tasks such as pick-and-place operations, assembly, sorting, and handling objects in unstructured environments.

The integration of locomotion and manipulation capabilities enables robots to perform complex tasks that require both mobility and manipulation skills. For example:

Search and Rescue: Robots equipped with both mobility and manipulation capabilities can navigate through disaster zones or hazardous environments to search for survivors while also manipulating debris or obstacles to access hard-to-reach areas [26].

Warehouse Automation: Robots in warehouse environments can navigate aisles to locate items, pick them up, and transport them to the desired location for sorting, packing, or shipping [16].

Construction and Maintenance in space: Construction and maintenance tasks in space are critical for the establishment and upkeep of infrastructure essential for space exploration and habitation. In these endeavors, robots play a pivotal role in executing various functions necessary for building, repairing, and maintaining space structures and facilities. These tasks include transporting construction materials, assembling intricate components, and conducting routine maintenance operations. Robots navigate through the unique challenges of the space environment, utilizing advanced technologies to maneuver, interact with, and manipulate tools and equipment. Through their capabilities, robots contribute to the ongoing development and sustainability of human presence and activities in space [47].

Assistive Robotics: In assistive applications, robots can provide mobility assistance to individuals with disabilities while also offering manipulation capabilities to help with tasks such as picking up objects, opening doors, or operating household appliances [11].

Integrating locomotion and manipulation capabilities in robots poses several technical challenges, including coordinating motion and manipulation actions, maintaining balance and stability during manipulation tasks, and adapting to changes in the environment. However, advancements in robotics technology, including improvements in sensors, actuators, and control algorithms, continue to enable the development of increasingly capable robots that can effectively combine locomotion and manipulation to perform complex tasks in diverse real-world scenarios.



Figure 1.2: Illustrates a hyper-redundant robot mounted on a mobile base from A. Wolf, et al., 2005 [96], in a search and rescue mission.

CHAPTER 1. INTRODUCTION

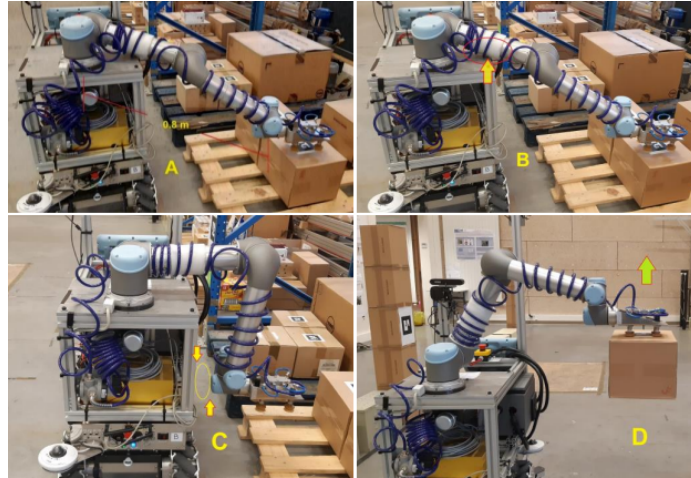


Figure 1.3: Illustrates robot in a warehouse, M. A. Khan, 2020, [34]

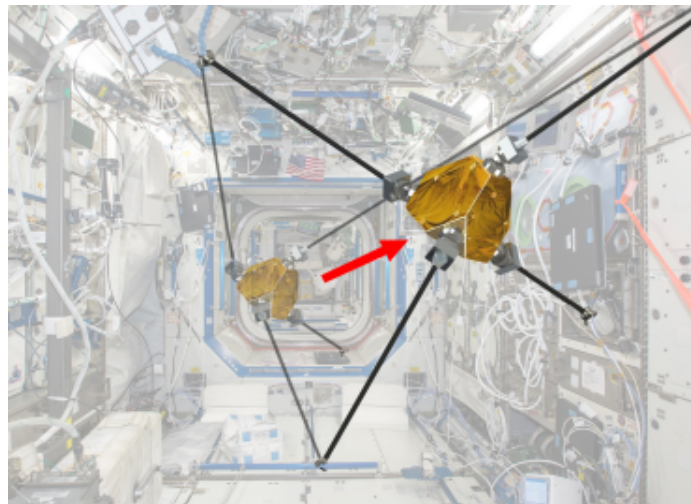


Figure 1.4: Illustrates robot navigating around space station, S. Schneider, et al., 2021, [67]

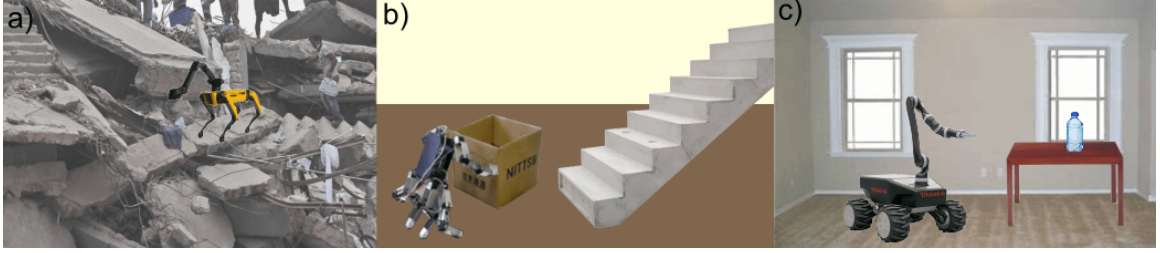


Figure 1.5: Challenges of loco - manipulation; a) shows the difficulty of navigating through clustered, narrow spaces [6]; b) shows the challenge of taking a box up a flight of stairs [32]; c) shows a wheeled manipulator trying to pick up an object during its locomotion [97].

1.1.1 Challenges in locomanipulation

Integrating locomotion and manipulation capabilities in robots presents several challenges, spanning technical, computational, and practical aspects. Some of the key challenges include:

1. **Coordination of Locomotion and Manipulation:** A major problem for solving locomotion challenge is to ensure stability of the robot during its interactions with environment. For instance, a legged robot has to make sure its projected center of mass should fall into the support polygon. On top of it, when combining manipulation tasks, the weight of the object has to be taken into consideration and made sure that the entire weight of the robot during this operation should be inside the support polygon to ensure stability. Also the contacts between the manipulator and the object should be well defined to ensure sufficient grasping even during locomotion of the mounted manipulator [24].
2. **Sensor Integration and Fusion:** Integrating locomotion and manipulation requires addition of multiple sensors in order to achieve efficiency. Sensors like Ultrasonic range finders, lidars can be used for estimating the distance from object, identifying obstacles; stereo cameras or 3D cameras can be integrated for localization of the mobile robot, integration of force and tactile sensors on manipulator joints to perfectly estimate the amount of force required to be applied to achieve necessary grasping. The challenge of having this type of multi-sensor fusion is due to the extremely dynamic nature of these mobile manipulators, there could be noise in data which gives rise to inaccurate measurements and error in precision during operation [100].
3. **Path Planning, Trajectory Optimization and Manipulation in Unstructured Environments:** Planning optimal paths for both locomotion and manipulation actions in complex

CHAPTER 1. INTRODUCTION

environments involves solving high-dimensional planning and optimization problems. Generating collision-free paths while considering constraints such as kinematic limits, environmental obstacles, and task requirements requires efficient algorithms capable of handling real-time planning and replanning. Manipulating objects in unstructured or cluttered environments, such as construction sites or disaster zones, presents additional challenges. Robots must be able to adapt their manipulation strategies to handle variations in object shape, size, weight, and location, as well as navigate through obstacles to reach target objects.

4. **Physical Interaction and Force Control:** Ensuring safe and effective physical interaction with objects during manipulation tasks requires precise force and torque control. Robots must be able to apply the right amount of force and pressure to grasp, lift, or manipulate objects without causing damage or instability. Developing robust control algorithms for force sensing and feedback control is essential for successful manipulation in diverse scenarios.
5. **Energy Efficiency and Payload Capacity:** Integrating locomotion and manipulation capabilities while maintaining energy efficiency and payload capacity is a significant challenge, especially for mobile robots or drones with limited onboard power and weight constraints. Optimizing the design and control of the robot's actuators, mechanisms, and power systems to minimize energy consumption while maximizing payload capacity is crucial for practical deployment in real-world applications.

1.2 Classification of Loco-Manipulation Approaches

1.2.1 Robot Arm Manipulators

There have been different manipulators in development over decades. Unimate introduced the first industrial robotic arm in 1961, it has subsequently evolved into the PUMA arm. This gave rise to further developments in robotic arms over the years [44]. Recent developments in these manipulators include having modifications in modelling to allow more flexibility and workspace. There are also various algorithms developed based on the environments in which these operate [66, 5]. Another development to these robotic arm manipulators is to have a moving base which increases the workspace [36, 9]. While these manipulators excel in tasks such as "pick and place" operations within controlled environments, they often fall short when extensive motion range is required. This is where loco-manipulation proves invaluable.



Figure 1.6: Classification of object manipulation approaches in the literature

1.2.2 Wheeled Mobile Manipulators

There are various methods of combining the task of manipulation to a mobile robot. Firstly we explore the straightforward way of achieving loco-manipulation - having a manipulator on a wheeled system [92] [3] . These systems provide sufficient stability during movement and a wide range of motion. Recent advancements also enable manipulation whilst moving. Despite its high feasibility, wheeled systems fail in highly unstructured environments and constrained spaces. They also introduce the problem of altering the environment due to their wheels which may not be desirable in all cases. This leads to exploring another method of incorporating manipulation on locomotors i.e. with the use of legged robots.

1.2.3 Legged Mobile Manipulators

Legged robots can have a unique role in manipulating objects in dynamic, human-centric, or otherwise inaccessible environments [24, 40]. They are more efficient in dodging obstacles as they can adjust their height and have fewer floor contact areas. There are multiple ways to use a legged system for object manipulation - 1. Passive manipulation i.e. pushing or kicking the object to



Figure 1.7: Illustrates Spot picking object from table [24]

desired location [32] [21], 2. Grasping with legs [28] [29] [69], 3. Attaching manipulators to the legged system, this is a more commonly used approach, for example Spotmini [25] and ANYmal [20] have been equipped with manipulators on their bodies to perform loco-manipulation tasks. One interesting robot is the TerminatorBot [93] which was specifically designed for the purpose of combining locomotion with manipulation. However these systems fail due to instability problems that may arise. If the legged system is designed to transform from purely legged configuration to manipulator + legged configuration, decreased contacts may make it unstable whereas if there is a separate manipulator attached to the legged system, there is a limit to the weight the manipulator can lift for it to maintain the entire center of mass within the support polygon to maintain stability.

1.2.4 Aerial Manipulators

To entirely eliminate these problems of having contacts with the environments one way to approach this problem is to have an aerial manipulator [33, 35]. Aerial manipulators encounter analogous challenges to those of UAVs, including nonlinearities, strong coupling, under-actuation, and susceptibility to disturbances [43]. In order to eliminate the above mentioned problems and increase versatility, continuum manipulators came into picture. These manipulators have a wide range of motion and due their flexible nature, they are not limited to operating conditions.



Figure 1.8: Illustrates a drone carrying packages [50]

1.2.5 Continuum Manipulators

Some research has been done on incorporating continuum manipulators on locomotive systems [37] [23] [27] [30]. Using a snake robot as a manipulator becomes an interesting task since due to its high dimensionality and slender structure, it can operate in any type of unstructured environment. [98] [18] [94]. Also the different gaits that can be implemented using snake-like locomotion on these robots gives flexibility in choosing the most energy efficient method in which the object can be manipulated [95, 41, 45, 39, 7, 68, 99, 61]. However, looking at the challenges faced by commonly used mobile manipulators and the problem we are trying to solve, using a snake robot for the purpose of object manipulation is the area I decided to explore.

1.3 Prior SS Lab Works

Before embarking on the creation of a versatile system adept at handling various locomotion and manipulation tasks, I drew inspiration from the diverse array of projects underway at Northeastern Silicon Synapse Lab. Engaging in control work on these projects equipped me with insights to tackle the locomotion and manipulation challenges, taking inspiration from biological systems [63, 65, 53, 42, 54, 71, 52]. At Northeastern, projects like Husky Carbon, a morphofunctional quadruped utilizing thrusters for stability in demanding environments [77, 82, 72, 12], and Harpy, a biped employing thruster-assisted walking, provided valuable reference points [73, 13, 46, 19, 12, 48]. Additionally, collaborative efforts with Caltech led to the development of the Multimodal Mobility

CHAPTER 1. INTRODUCTION

Morphobot (M4), capable of seamlessly transitioning between aerial and wheeled locomotion [82, 83, 81, 38]. Northeastern’s Aerobat showcased proficiency in navigating confined spaces where traditional drones struggle due to rotor-induced backdraft [76, 75, 80, 91, 84, 74, 85, 79]. Across all these platforms, robust control strategies are imperative, facilitating effective planning and seamless morphing between different locomotive configurations.

1.4 COBRA Design Motivation

Snake robots have undergone over three decades of development, largely due to their adaptable nature across various applications. This prompted the creation of COBRA specifically for NASA’s BIG Idea competition. In 2022, NASA’s Innovative Advanced Concepts (NIAC) Program invited academic institutions in the United States to participate in NASA’s Breakthrough, Innovative, and Game-changing (BIG) Idea competition, with a focus on pioneering mobility solutions capable of traversing lunar craters. Northeastern University clinched NASA’s prestigious Artemis Award in this competition with a groundbreaking proposal introducing an articulated robot tumbler named COBRA (Crater Observing Bio-inspired Rolling Articulator). COBRA employs sidewinding motion to approach the crater, transforms into a wheel configuration, and utilizes gravitational forces to descend into the crater, thereby establishing an energy-efficient system while ensuring stability. These distinctive attributes of COBRA render it applicable across diverse domains, including search and rescue operations, inspection within confined spaces, and the manipulation of objects in cluttered environments.

1.5 Loco-manipulation using COBRA

Although using a snake robot as a manipulator is an explored avenue, what makes this thesis novel is the design of COBRA itself. Most of the snake robots in existence either have wheels or do not have the capability of grasping onto an object and moving around. The existence of wheels defeats the purpose of operating in unstructured environments. The absence of wheels on COBRA and the ability for it to latch onto objects makes it easier to develop gaits which can hold on to objects of different shapes and sizes and move those objects around in different environments with rough terrains or inclines.

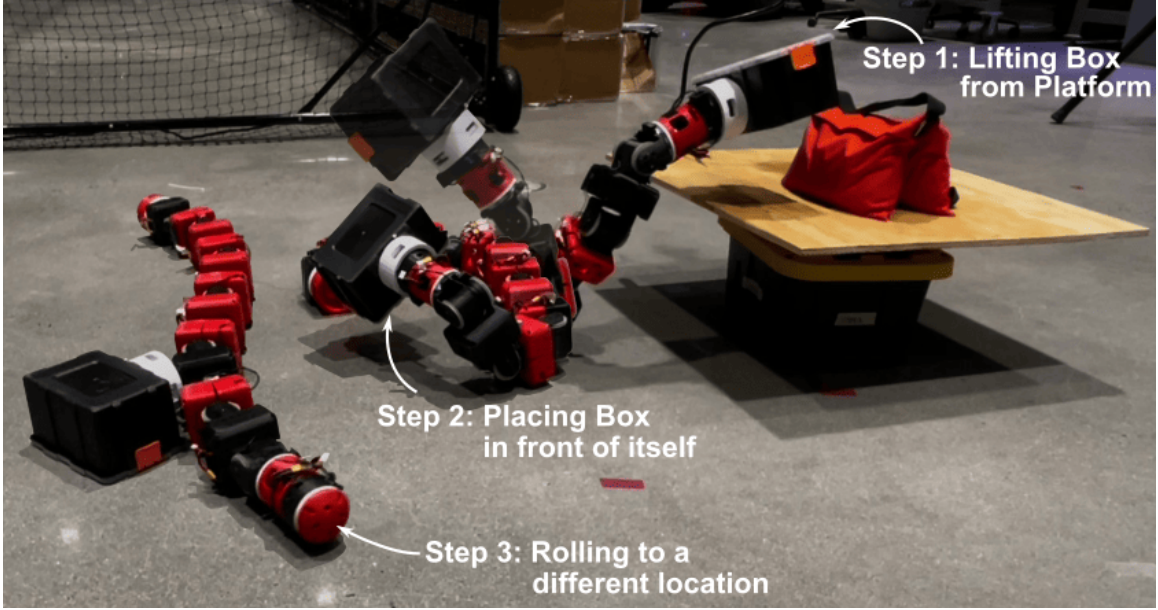


Figure 1.9: Object manipulation using COBRA

1.6 Objectives and Outline of Thesis

Optimization-driven path planning and control strategies have emerged as pivotal methodologies for managing diverse contact-intensive systems within real-world experimental settings. These approaches have found widespread application across various locomotion modalities, such as legged and slithering locomotion, showcasing remarkable efficacy, including rapid contact planning in terrestrial environments [14, 8, 15]. Notably, point-contact models such as legged robots have been particularly receptive to optimization techniques [87] [1] compared to systems characterized by extensive contact interactions, such as snake robots. Given the intricate dynamics inherent in slithering systems, which encompass sophisticated contact dynamics [22, 10, 88], there arises a pressing need for enhanced modeling and control methodologies. These tools are indispensable for orchestrating body movements through the modulation of joint torques, ground reaction forces, and the coordination of contact sequences comprising timing and spatial positioning. Addressing this contact-rich problem presents intriguing prospects for leveraging contact-implicit optimization, which represents a prevalent design paradigm in the field of locomotion and for unknown reasons is less explored in snake-type robots. The primary research objectives encompass: Investigating optimal control design approaches to effectively guide the joints along desired trajectories for object manipulation. This work introduces an optimization approach based on non-impulsive contact-implicit path

CHAPTER 1. INTRODUCTION

planning for COBRA. We demonstrate the effectiveness of this method in generating optimal joint trajectories for desired object movements across flat and ramp surfaces in simulation and experiment [49, 62, 89, 70].

1.7 Contributions

In this thesis, I demonstrated the application of COBRA within the Simscape model to manipulate objects through various methods. The research showcases the manipulation of boxes with differing weights, both on level ground and a sloped ramp. Through meticulous experimentation, it is illustrated that COBRA exhibits proficiency in lifting boxes and relocating them onto raised platforms, and conversely, transferring them from elevated positions to ground level. The experiments conducted within the simulation environment were meticulously replicated on physical COBRA hardware, yielding consistent results. This process not only validates the efficacy of COBRA within a virtual setting but also underscores its practical applicability in real-world scenarios. The study underscores the versatility of COBRA in object manipulation tasks, demonstrating its adaptability to diverse environments and scenarios. By showcasing its capabilities across simulated and physical domains, the research bridges the gap between theoretical simulations and practical implementations. Furthermore, the successful replication of results on physical hardware reaffirms the reliability and robustness of COBRA-based manipulation techniques. This not only bolsters confidence in the simulation-based findings but also instills trust in the potential deployment of COBRA in real-world applications requiring precise object manipulation. Overall, my thesis contributes to the understanding of COBRA's capabilities within object manipulation, providing valuable insights for both theoretical modeling and practical implementation. Through meticulous experimentation and validation, it demonstrates the effectiveness of COBRA across simulated and physical environments, paving the way for its utilization in various industrial and robotic applications.

Chapter 2

COBRA Platform

2.1 COBRA Hardware

COBRA has 11 degrees of freedom that enables the robot to change into different shapes enabling different modes of locomotion. In snake mode, our system will utilize sidewinding for movement on flat or uphill terrain. Sidewinding is a type of snake locomotion used to move across loose or slippery surfaces such as sand. The symmetry of the modules allows us to make COBRA roll in various directions without having to make any modifications to the module design. It can also enter the tumbling mode by connecting the head and tail of the system together.

A modular system provides many benefits for operation, design, and manufacturability. The goal is that each joint module is simple and interchangeable, allowing for rapid prototyping and building of the system. As shown in Fig. 2.2 below, a single module of COBRA has 1 degree of freedom joint that can rotate a full 180 degrees. In addition, each module has a circular female connector on one end and a male connector on the other. This way the modules can be attached in different configurations. The system will consist of 10 joint modules alternately connected. The 11th module is the tail module which is designed to latch onto the head module to morph into the tumbling configuration. The entire system weighs only 6 kg, with a diameter of 10 cm and length of 1.6 meters.

The joint modules utilize XW series motors from DYNAMIXEL. These off-the-shelf servo motors are already integrated with a controller, driver, encoder, reduction gear, and RS-485 network communication. The XW series also have IP68 certified ingress protection from dust and are waterproof to depths of 1 meter. The power and communication for these motors are daisy chained and controlled by a single Raspberry Pi computer located in the head module of the system. This

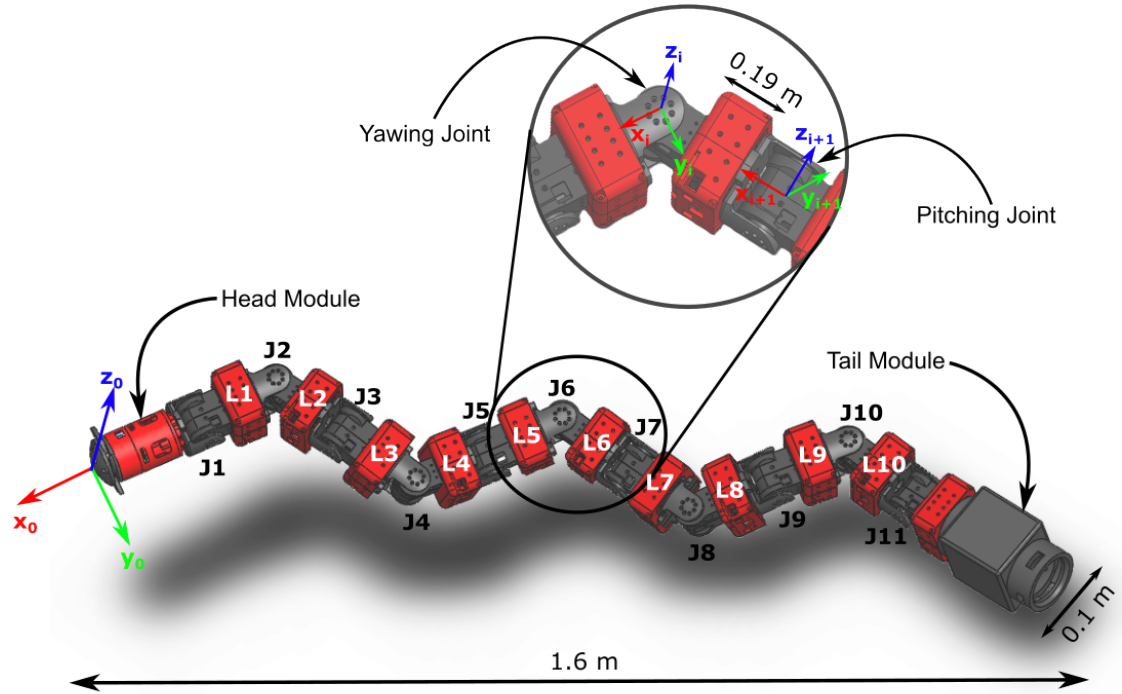


Figure 2.1: This image shows the overview of COBRA model with the head coordinate frame and the coordinate frames for the yawing and pitching joints which are consistent throughout the robot. It also show the naming convention used accross all the models and codes in which Jx corresponds to the joints and Ly corresponds to the link where x ranges from 1 to 11 and y ranges from 1 to 10, excluding the head and tail.

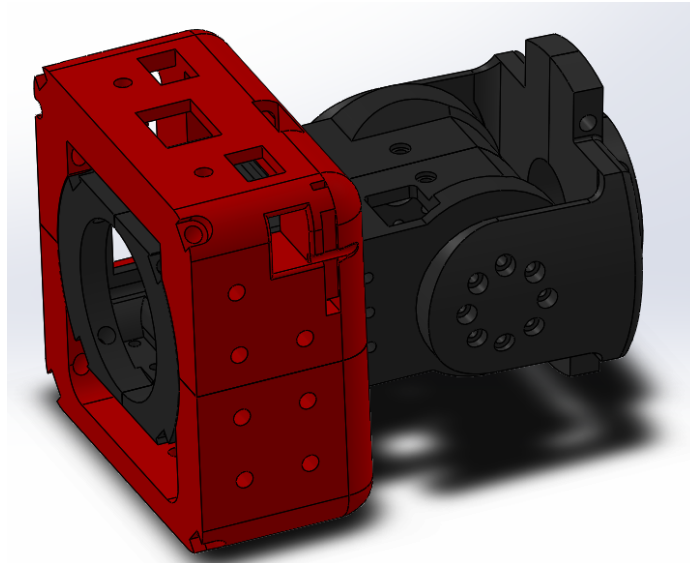


Figure 2.2: A single COBRA module

makes it quicker to set up compared to a more custom motor solution. The joint module housing is fabricated using a Markforged carbon fiber reinforced nylon, which allows for extremely strong and lightweight modules. The design of the joint modules is driven by the worst-case loading scenario of transforming into and out of tumbling mode, which requires 6.9 Newton-meters of torque.

In addition to the eleven identical modules, COBRA features a distinct module at the snake's head, aptly referred to as the "head module," and similarly, a "tail module" at the snake's tail end. The head module is shown in Fig. 2.3 . The primary purpose of these unique modules are to connect together to form a loop prior to the onset of tumbling mode. The head module acts as the male connector and utilizes a latching mechanism to sit concentrically inside the female tail module. The latching mechanism consists of a Dynamixel XC330 actuator, which sits within the head module and drives a central gear. This gear interfaces with the partially geared sections of four fin-shaped latching "fins." The curved outer face of each latching fin has an arc length equal to 1/4 of the circumference of the head module's circular cross-section. When the mechanism is retracted, these four fins form a thin cylinder that coincides with the head module's cylindrical face. A dome-shaped cap lies on the end of the head module so that the fins sit between it and the main body of the head module. Clevis pins are used to position the fins in this configuration. COBRA's tail module features a female cavity for the fins. When transitioning to tumbling mode, the head module is positioned concentrically inside the tail module using the joint's actuators, and the fins

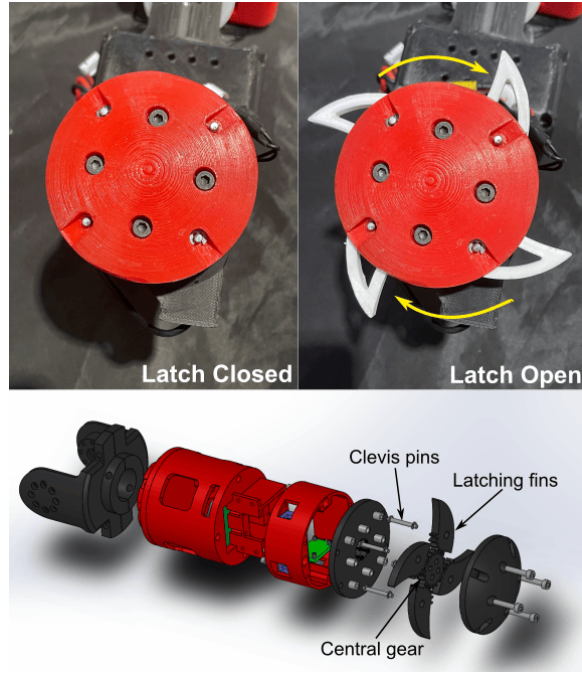


Figure 2.3: (Above) Closeup view of the head with actuated fins. (Below) Expanded view of the head module.

unfold into the cavity to lock the head module in place. For the head and tail modules to unlatch, the central gear rotates in the opposite direction, and the fins retract, allowing the system to return to sidewinding mode. The choice for an active latching mechanism design stemmed from the design requirements and restrictions. Magnets were initially discussed as a passive latching option, however they would not be effective in conjunction with the ferromagnetic regolith. Further, due to the need to stay in a latched configuration even when a large amount of force is applied to the system during tumbling, a passive system was not chosen, for there would be the risk of unlatching during tumbling. An attachment similar to the tail module was made for the box as a docking module 2.4. This entire mechanism is useful for the loco-manipulation problem which will be discussed further.

2.2 Simulation Setup

Multibody simulation plays a pivotal role in addressing kinematic and dynamic challenges. Its application spans across a wide spectrum, encompassing everything from individual mechanical components, to complex mechanisms, and even robotic systems. The multibody model of a mechanical system is structured around rigid and deformable bodies, interconnected via kinematic pairs.

CHAPTER 2. COBRA PLATFORM



Figure 2.4: (Above) Docking module on the box. (Below) Head module latched onto the docking module on the box.

These bodies are capable of experiencing substantial translational and rotational displacements. The primary parameters utilized for characterizing bodies within the multibody simulator encompass: a local reference frame with its origin situated at the body's center of mass and aligned with its principal axes, the mass, the inertia tensor within the local reference frame, and additional auxiliary references for delineating constraints, represented through interrelations among motion parameters. Both rigid and flexible bodies are depicted using singular or combinations of multiple blocks to portray their mechanical characteristics. The interconnection of all bodies occurs through joints or appropriate constraints, creating an assembly of an articulated mechanism. The resulting degrees of freedom stem from the kinematic relationships established by the constraint blocks. There are several tools available to create a simulation model. We are using the MATLAB *Simulink Multibody Toolbox* to create a high fidelity simulation for COBRA simulation model.

2.2.1 Actuator model

Each link is represented as a rigid body with a mass of 0.5 kg, and the inertia matrices are automatically computed by MATLAB based on the geometry, assuming a uniform mass distribution. These geometries are obtained as meshes imported from the SolidWorks model for each link. We use the convex hull of these imported geometries which facilitates modeling contacts between surfaces. The inertia and mass information of these geometries are directly imported from the mesh

CHAPTER 2. COBRA PLATFORM

files. The inertia tensor for each of the ten identical body links is as follows: ($\mathbf{I}_{xx} = 7.167 \times 10^{-4}$, $\mathbf{I}_{yy} = 8.704 \times 10^{-4}$, $\mathbf{I}_{zz} = 8.626 \times 10^{-4} \text{ kgm}^2$), and the inertia tensors for the head and tail modules are ($\mathbf{I}_{xx} = 4.4562 \times 10^{-4}$, $\mathbf{I}_{yy} = 1.710 \times 10^{-3}$, $\mathbf{I}_{zz} = 1.793 \times 10^{-3} \text{ kgm}^2$) and ($\mathbf{I}_{xx} = 8.182 \times 10^{-4}$, $\mathbf{I}_{yy} = 1.141 \times 10^{-3}$, $\mathbf{I}_{zz} = 1.109 \times 10^{-3} \text{ kgm}^2$) along the primary axes and the mass of each module is taken to be roughly 0.5 g. Each link is connected via position-controlled revolute joints, with the axes of these joints defined using the Denavit-Hartenberg parameters. The joint restricts the movement of two arbitrary frames linked to the base and follower frames, allowing only pure rotation along a shared axis. This axis of rotation coincides with the z-axis of the joint's base frame. Both the base and follower frames share the same origin and z-axis. The follower frame rotates around the z-axis. The revolute joint block facilitates the replication of actual motor parameters on the robot by adjusting internal mechanical parameters and setting actuation limits to restrict joint movement. In our model, we have specified actuation upper and lower bounds with limiting position values ranging from -90° to 90° , spring stiffness value to $1 \times 10^4 \text{ Nm/deg}$ and damping coefficient to 10 Nms/deg . Additionally, the revolute joint block enables us to activate sensing from the joints, allowing measurement of joint angles, velocities, accelerations, and torques. This capability enables us to compare the results obtained from our Simscape simulation with the values obtained from our robot actuators. This setup gives us the COBRA simscape model which can be used for various experiments. Along with this, we designed a latch joint using the weld joint which enables engaging and disengaging a joint while the simulation is running. We have a 6 DOF joint modelling between the head frame and the ground frame which enables motion of COBRA with respect to the ground. We can extract the position data from the frames between each link by connecting it to the transform sensor. This transform sensor is connected between the frame of each link and the ground frame. The measurement frame option on the sensor allows us to opt any frame with reference to which we want to obtain the measured data in. The selection of the measurement frame does not affect the rotational quantities. The Transform Sensor block has five different options for the Measurement Frame parameter. We selected the measurement frame to be the base frame which is the ground frame in our application. We enabled sensing for the transform sensor to collect data for rotational transform, positions velocities, accelerations, angular velocities and angular accelerations in xyz directions. We have this entire actuator model setup as a library block which allows us to setup various simscape models without having to develop the same actuator repeatedly.

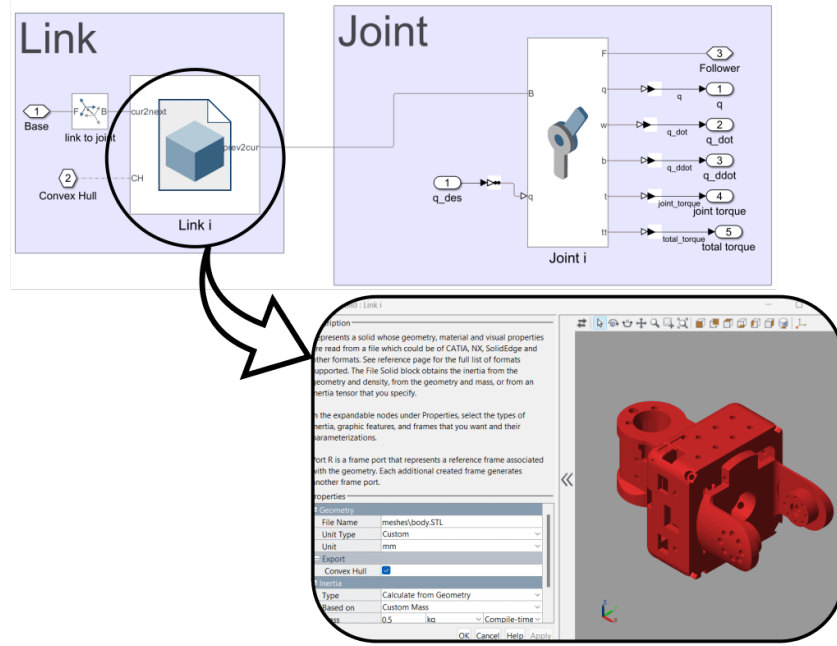


Figure 2.5: Simscape block for actuator model

2.2.2 Contact force model

The interactions between surfaces of solids is an important aspect in any Multibody simulator. This can be done in Simscape using the Simscape spatial contact force block. This block allows to develop a contact model between a pair of bodies. The Spatial Contact Force block models the contact between a pair of geometries in 3-D space. It uses the Kelvin-Voigt model to model contacts. The model adopts a regularization method, alternatively referred to as compliance or viscoelasticity, wherein the interacting bodies are treated as deformable within the contact region. Consequently, the contact forces can be described as a continuous function of the localized deformation occurring between the contacting surfaces [49] [86]. Throughout contact, each geometry possesses a dedicated contact frame situated precisely at the contact point. These contact frames consistently coincide and define the contact plane through their xy-planes. Notably, the z-direction of these frames serves as an outward normal vector for the base geometry and an inward normal vector for the follower geometry. As continuous contact ensues, the contact frames dynamically shift along the geometry, tracking the movement of the contact point. The block applies contact forces to the geometries at the origin of the contact frames in accordance with Newton's Third Law: The normal force, f_n , which is aligned with the z-axis of the contact frame. This force

CHAPTER 2. COBRA PLATFORM

pushes the geometries apart in order to reduce penetration; The frictional force, f_f , which lies in the contact plane. This force opposes the relative tangential velocities between the geometries. The normal forces for all contact interactions between robot links, ground surface and object are modeled using a *Smooth Spring-Damper* model with spring stiffness $1 \times 10^{-4} \text{ N/m}$, damping coefficient $1 \times 10^3 \text{ Ns/m}$ and a transition width of $1 \times 10^{-3} \text{ m}$. Transition width characterises the transitional region to force equations. By varying the transition width we can achieve sharper transitions for lower values and smoother for higher values. The normal force is calculated by:

$$f_n = s(d, w) \cdot (k \cdot d + b \cdot d')$$

where,

- f_n is the normal force applied in equal-and-opposite fashion to each contacting geometry.
- d is the penetration depth between two contacting geometries.
- w is the transition region width specified in the block.
- d' is the first time derivative of the penetration depth.
- k is the normal-force stiffness specified in the block.
- b is the normal-force damping specified in the block.
- $s(d, w)$ is the smoothing function.

Friction forces are modeled using a *Smooth Stick-Slip* model with coefficient of static friction of 0.7, coefficient of dynamic friction of 0.5 and critical velocity $1 \times 10^{-3} \text{ m/s}$. The stick-slip friction force is calculated by:

$$|f_f| = \mu \cdot |f_n|$$

where,

- f_f is the frictional force.
- f_n is the normal force.
- μ is the effective coefficient of friction.

At high relative velocities, the value of the effective coefficient of friction is close to that of the coefficient of dynamic friction. At the critical velocity, the effective coefficient of friction achieves a maximum value that is equal to the coefficient of static friction. From this block we can output contact information such as contact signal, penetration and separation distances, normal and friction force, relative normal velocity and relative tangential velocity, and rotations and translations of the follower and base frames. For our implementation, we are only sensing contact signal, normal and friction force, relative tangential velocity and follower frame rotation and translation. The contact

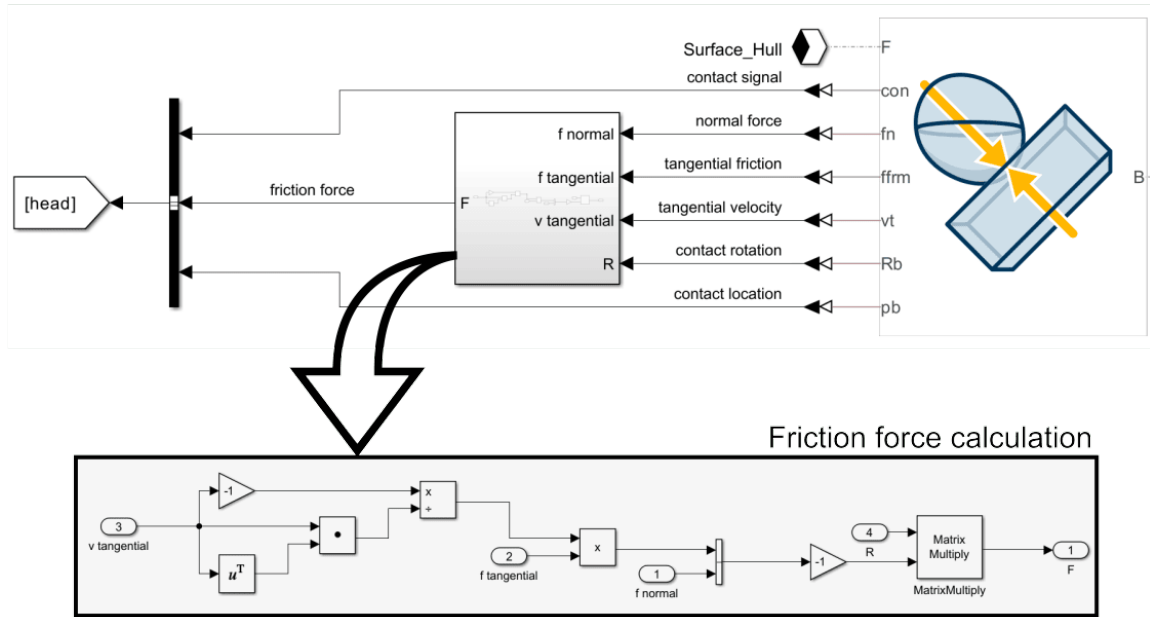


Figure 2.6: Simscape contact force block

signal gives a binary output; 0 if there's no contact or 1 during contacts. The detected friction force is a $1 \times N$ matrix which just gives us the magnitude of the force. We use the tangential velocity vector, which is a $2 \times N$ matrix, to get the unit vector which can be multiplied to get the friction force components, which when concatenated with the normal force ($1 \times N$ matrix) gives us a $3 \times N$ matrix of contact forces between any two surfaces. This is then rotated to the ground frame to help us analyse contact data and visualise it better. We set this entire model as a library block which becomes easier to make uniform changes across all the simulation environments we have set up for different experiments.

2.2.3 Environment setup for Loco-manipulation

Using the actuator model library block and the contact model library block, we can create simulation environments for our experimentation. We can directly connect the robot body hulls and the ground hull to the contact model block to model contacts between robot and ground and simultaneously output the contact data to Matlab workspace for further analysis. We have different output variables to store data for robot contacts with ground, box contacts with ground, robot contacts with box, robot joint data, robot pose data and box pose data. Considering the accuracy of Simscape model to match the actual robot movement, it becomes crucial to collect contact information and

CHAPTER 2. COBRA PLATFORM

to true data from our Simscape model since we don't have any IMUs or Force sensors on our hardware yet. We use the data we get from our Simscape model for contact model analysis. We can change the initial pose of the robot as per our requirements. In case of lateral rolling or sidewinding gaits we have the robot oriented in a way that the yawing joints are parallel to the ground plane. In case of our loco-manipulation gaits, we rotated the robot by 90° . For setting up the environment for loco-manipulation, we have a model which contains the object, the platform and the ramp. The object being manipulated is modeled as a solid box of weight 0.5 kg, with a replica of the tail module attached to the side of the box. The head module latches onto this module on the box while performing tasks like placing the box on the platform or picking the box from the platform. We have a similar setup to model contacts between the box and the ground. We also have a contact model which gives us information of contacts between the robot and the box which allows us to estimate which modules of COBRA are in contact with the box during locomotion for different gaits which gives us another metric to compare the gaits. The platform used to pick/place the box is placed at a height of 0.3 m and the ramp is inclined at an angle of 16.7° with maximum elevation of 0.6 m. These both are modelled as solid objects with fixed positions with respect to the ground frame. We also have a separate contact model library block for the ramp with the robot and the box each. All these blocks are connected to an inertial frame (which is the ground frame in our case), a uniform gravity block with a constant acceleration of gravity of 9.8 m/s^2 in the negative z axis, and a solver configuration block. Each physical network represented by a connected Simscape™ block diagram requires solver settings information for simulation. The Solver Configuration block specifies the solver parameters that your model needs before you can begin simulation. We have the Equation Formulation (specifies how solver treats sinusoidal variables) setup at Frequency and Time which makes the simulation faster, a consistency solver factor of 1×10^{-9} provides a scaling factor for determining how accurately the algebraic constraints are to be satisfied at the beginning of simulation and after every discrete event and by keeping the "Apply filtering at 1-D/3-D connections when needed" box checked, the solver automatically applies input filtering to the signal entering the Simulink-PS Converter block to obtain this additional derivative with a filtering time constant parameter of 0.001 which provides the time constant for the delay. A solver applies a numerical method to solve the set of ordinary differential equations that represent the model. Through this computation, it determines the time of the next simulation step. In the process of solving this initial value problem, the solver also satisfies the accuracy requirements that you specify. An extensive set of fixed-step and variable-step continuous solvers are provided in Simscape, each of which implements a specific ODE solution method. The appropriate solver for simulating a model depends System

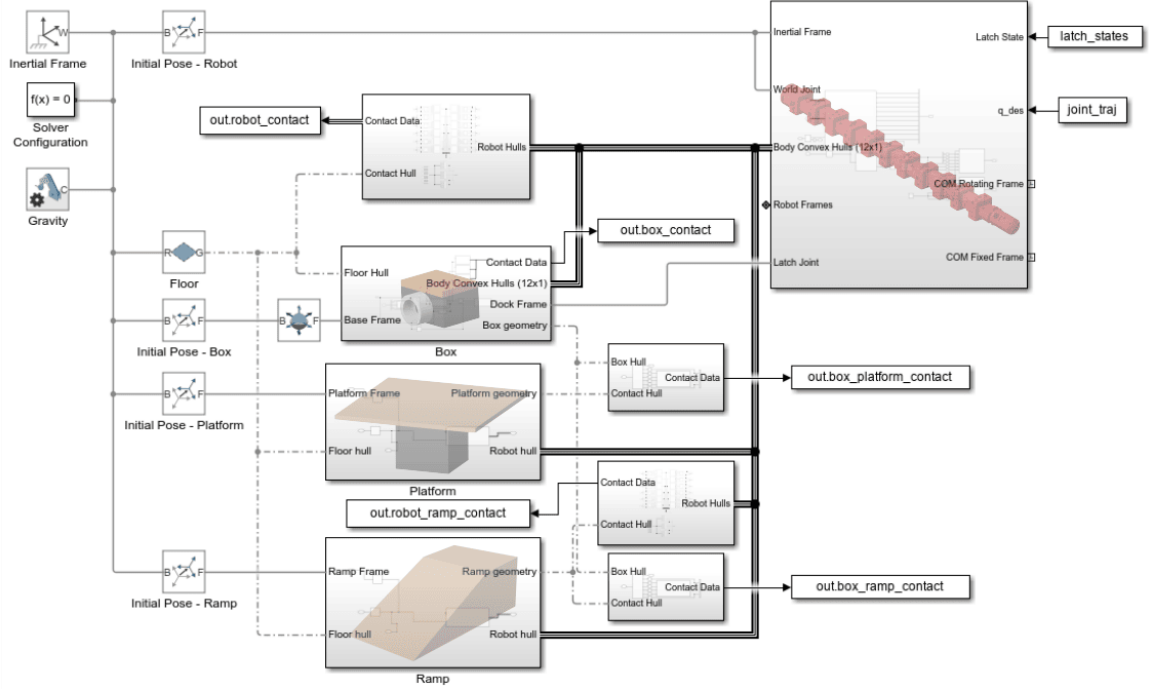


Figure 2.7: Simscape model setup

dynamics, Solution stability, Computation speed, Solver robustness. By choosing the auto-solver, Simscape picks the best numerical method and a fixed timestep depending on the given model. In case the solver is not satisfactory, we have the freedom of choosing our own numerical integration method and timestep value in the solver configurations. For our model, we have auto-solver where the dynamics are solved using MATLAB's *ode45* with a fixed timestep of 1×10^{-4} seconds which are the default settings. We implemented a variable step solver for our model but it seemed to slow down the simulation. Even with the auto-solver setup, the total simulation time varies depending on the contacts, the more number of contacts we have defined in our model, the slower the simulation runs. We can speed up the simulation by increasing the timestep but it affects the accuracy of simulation which may not be a desirable tradeoff considering the data we use for analysis.

2.3 Open-loop CPG gaits

The COBRA hardware currently doesn't support a closed loop controller. In order to achieve desired movements we generate gaits on our COBRA model using an open-loop Central Pattern Generator (CPG). CPG produces a rhythmic output for a fixed given input. We use the same

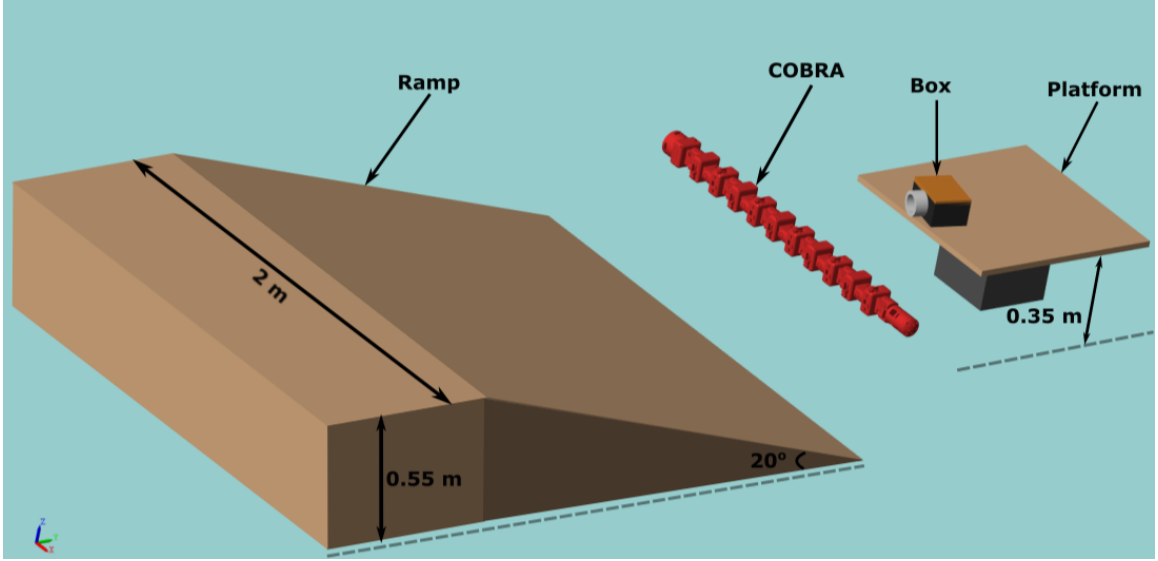


Figure 2.8: Simscape environment setup for loco-manipulation problem

parameters in our simscape model and hardware. The simscape model gives a good approximation to the feasibility of a certain gait which can then be directly implemented on our hardware with a high accuracy. We generate gaits using a sinusoidal wave at each joint with fixed values for amplitude, frequency and phase angles. By varying these CPG parameters we obtain different gaits. After observing the sidewinding gaits in snakes, we determined that the same can be replicated by having one sinusoidal wave which passes through the body in a plane parallel to the ground and another sinusoidal wave in a plane perpendicular to the ground and parallel to the direction of locomotion. The horizontal sine wave (in the plane parallel to ground) is the one that drives the robot to move forward whereas the sine wave in the vertical plane enables alternating anchor points. Implementing these simultaneously generates a gait which imitates sidewinding in snakes. For sidewinding (shown in Fig. 2.9), we have an amplitude of 60° for yawing joints and 14° for pitching joints, frequency of 0.5 and phase angles $\pi/2 * [0, 0, 1, 1, 2, 2, 3, 3, 0, 0, 1]$. In case of lateral rolling, all the joints in the same plane needed to move at the same time and the moment the robot flips by 90° , the alternate joints should carry on the same movement. We have a sine wave that goes through all yawing joints simultaneously with no phase difference between them and have the same sine wave go through the pitching joints after one wave cycle, hence the yawing and pitching joints have a phase difference of $\pi/2$. The amplitude for this gait controls the shape of the lateral rolling which can be adjusting according to the environments that the COBRA operates in and the application for which we are using COBRA. For rolling gaits, we have the same amplitude of 20° for

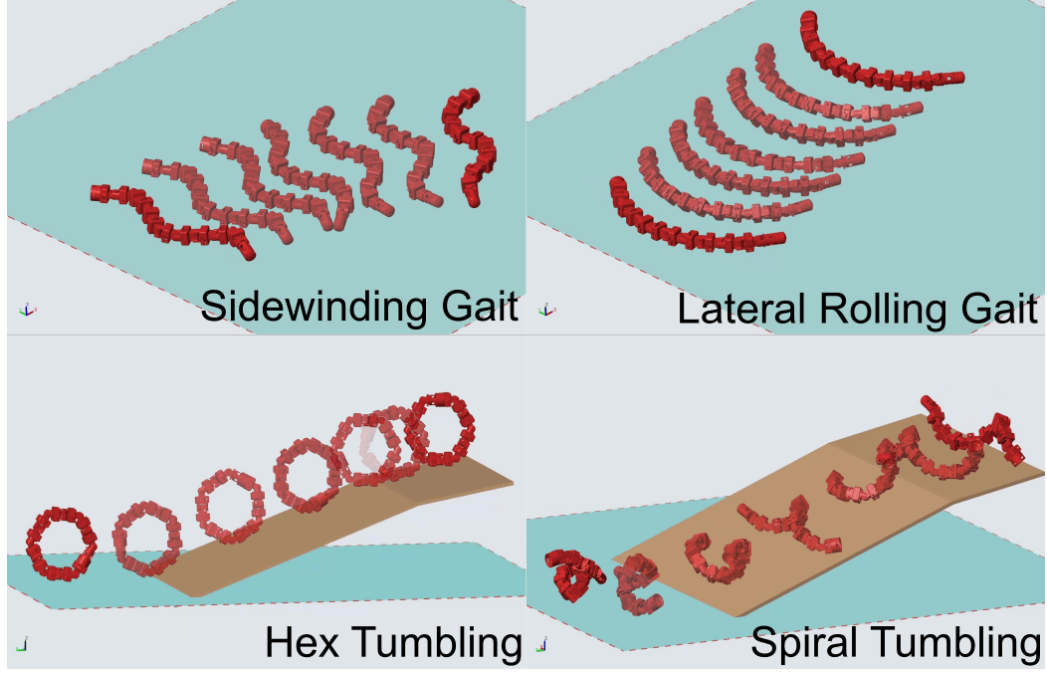


Figure 2.9: Various gaits implemented on COBRA

a C-shape lateral rolling (depicted in the Fig. 2.9) for pitching and yawing joints, a phase difference of $\pi/2 * [0, 1, 0, 1, 0, 1, 0, 1, 0, 1, 0]$. We also have fixed angles which makes the COBRA go into the spiral configuration or the hex configuration which were determined by simple geometry (shown in Fig. 2.9). These gaits are used for rolling down the slope without having to actively engage joints and conserving energy.

Chapter 3

Contact Modelling

The motion dynamics governing the COBRA snake robot, equipped with 11 body joints, are succinctly captured in the following equations of motion [64]:

$$\begin{aligned} M(\mathbf{q})\dot{\mathbf{u}} - \mathbf{h}(\mathbf{q}, \mathbf{u}, \boldsymbol{\tau}) &= \sum_i \mathbf{J}_i^\top(\mathbf{q}) \mathbf{f}_{ext,i}, \\ \mathbf{h}(\mathbf{q}, \mathbf{u}, \boldsymbol{\tau}) &= \mathbf{C}(\mathbf{q}, \mathbf{u})\mathbf{u} + \mathbf{G}(\mathbf{q}) + \mathbf{B}(\mathbf{q})\boldsymbol{\tau} \end{aligned} \quad (3.1)$$

In this expression, the mass-inertia matrix \mathbf{M} operates in a space of dimensionality $\mathbb{R}^{17 \times 17}$, the terms encompassing centrifugal, Coriolis, gravity, and actuation ($\boldsymbol{\tau}$) are succinctly represented by $\mathbf{h} \in \mathbb{R}^{17}$, the external forces $\mathbf{f}_{ext,i}$ and their respective Jacobians \mathbf{J}_i reside in the space $\mathbb{R}^{3 \times 17}$.

In the object manipulation problem depicted in Fig. 3.1, the external forces stem solely from active unilateral constraints, such as contact forces between the ground surface and the robot or between a movable object and the robot. This assumption conveniently establishes a complementary relationship, where the product of two variables, including force and displacement, in the presence of holonomic constraints is zero, between the separation \mathbf{g}_i (the gap between the body, terrain, and object) and the force exerted by a hard unilateral contact.

The concept of normal cone inclusion on the displacement, velocity, and acceleration levels from [90] permits the expression:

$$\begin{aligned} -\mathbf{g}_i &\in \partial\Psi_i(\mathbf{f}_{ext,i}) \equiv \mathcal{N}_{\mathcal{F}_i}(\mathbf{f}_{ext,i}) \\ -\dot{\mathbf{g}}_i &\in \partial\Psi_i(\mathbf{f}_{ext,i}) \equiv \mathcal{N}_{\mathcal{F}_i}(\mathbf{f}_{ext,i}) \\ -\ddot{\mathbf{g}}_i &\in \partial\Psi_i(\mathbf{f}_{ext,i}) \equiv \mathcal{N}_{\mathcal{F}_i}(\mathbf{f}_{ext,i}) \end{aligned} \quad (3.2)$$

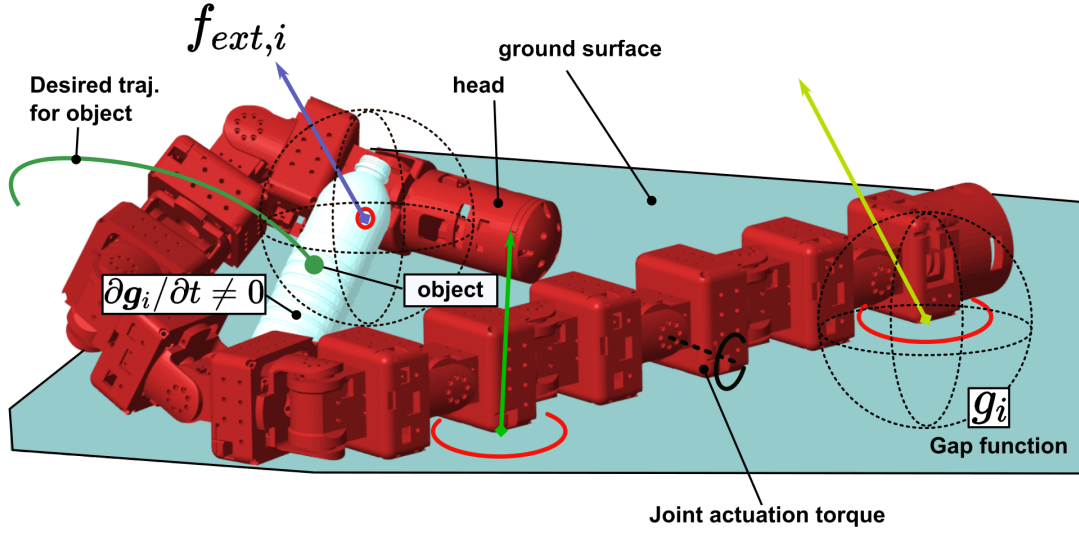


Figure 3.1: Full-dynamics model parameters in the object manipulation task considered in this paper

where $\Psi_i(\cdot)$ denotes the indicator function. The gap function g_i is defined such that its total time derivative yields the relative constraint velocity $\dot{g}_i = \mathbf{W}_i^\top \mathbf{u} + \zeta_i$, where $\mathbf{W}_i = \mathbf{W}_i(\mathbf{q}, t) = (\partial g_i / \partial \mathbf{q})^\top$ and $\zeta_i = \zeta_i(\mathbf{q}, t) = \partial g_i / \partial t$.

In the context of the primary objectives of loco-manipulation with COBRA, various conditions of the normal cone inclusion as described in Eq. 3.2 were explored. In scenarios where nonimpulsive unilateral contact forces are employed to manipulate rigid objects (e.g., the box shown in Fig. 3.1), $\partial g_i / \partial t \neq 0$. This factor holds significant importance in motion planning considered in this work and is enforced during optimization.

The total time derivative of the relative constraint velocity yields the relative constraint accelerations $\ddot{g}_i = \mathbf{W}^\top \dot{\mathbf{u}} + \hat{\zeta}_i$ where $\hat{\zeta}_i = \hat{\zeta}_i(\mathbf{q}, \mathbf{u}, t)$. We describe a geometric constraint on the acceleration level such that the initial conditions are fulfilled on velocity and displacement levels:

$$\begin{aligned}
 g_i(\mathbf{q}, t) &= 0, \\
 \dot{g}_i &= \mathbf{W}_i^\top \mathbf{u} + \zeta_i = 0, \\
 \ddot{g}_i &= \mathbf{W}_i^\top \dot{\mathbf{u}} + \hat{\zeta}_i = 0, \\
 \dot{g}_i(\mathbf{q}_0, \mathbf{u}_0, t_0) &= 0, \\
 \partial g_i / \partial t &\neq 0
 \end{aligned} \tag{3.3}$$

which implies that the generalized constraint forces must be perpendicular to the manifolds $g_i = 0$, $\dot{g}_i = 0$, and $\ddot{g}_i = 0$. This formulation directly accommodates the integration of friction laws, which

CHAPTER 3. CONTACT MODELLING

naturally pertain to velocity considerations. We divide the contact forces into normal and tangential components, denoted as $\mathbf{f}_{ext,i} = \begin{bmatrix} f_{N,i} & \mathbf{f}_{T,i}^\top \end{bmatrix}^\top \in \mathcal{F}_i$.

In this context, the force space \mathcal{F}_i facilitates the specification of non-negative normal forces (\mathbb{R}_0^+) and tangential forces adhering to Coulomb friction $\{\mathbf{f}_{T,i} \in \mathbb{R}^2, \|\mathbf{f}_{T,i}\| < \mu |f_{N,i}|\}$, with μ representing the friction coefficient.

The underlying rationale behind this approach is that while the force remains confined within the interior of its designated subspace, the contact velocity remains constrained to zero. Conversely, non-zero gap velocities only arise when the forces reach the boundary of their permissible set, indicating either a zero normal force or the maximum friction force opposing the direction of motion.

To proceed with the loco-manipulation problem considered here, it proves advantageous to reconfigure Eq. 3.1 into local contact coordinates (task space). This can be achieved by recognizing the relationship:

$$\dot{\mathbf{g}} = \mathbf{J}_c \mathbf{u}, \quad (3.4)$$

where \mathbf{g} and \mathbf{J}_c represent the stacked contact separations and Jacobians, respectively. By differentiating the above equation with respect to time and substituting Eq. 3.1, we obtain:

$$\ddot{\mathbf{g}} = \mathbf{J}_c \mathbf{M}^{-1} \mathbf{J}_c^\top \mathbf{f}_{ext} + \dot{\mathbf{J}}_c \mathbf{u} + \mathbf{J}_c \mathbf{M}^{-1} \mathbf{h}, \quad (3.5)$$

where $\mathbf{G} = \mathbf{J}_c \mathbf{M}^{-1} \mathbf{J}_c^\top$ – the Delassus matrix – signifies the apparent inverse inertia at the contact points, and $\mathbf{c} = \dot{\mathbf{J}}_c \mathbf{u} + \mathbf{J}_c \mathbf{M}^{-1} \mathbf{h}$ encapsulates all terms independent of the stacked external forces \mathbf{f}_{ext} . At this point, the principle of least action asserts that the contact forces are determined by the solution of the constrained optimization problem:

$$\begin{aligned} & \underset{\{\mathbf{f}_{ext,i}, \mathbf{u}\}}{\text{minimize}} \quad \frac{1}{2} \mathbf{f}_{ext}^\top \mathbf{G} \mathbf{f}_{ext} + \mathbf{f}_{ext}^\top \mathbf{c} \\ & \text{s.t.} \\ & \text{(1)} \quad \mathbf{M}(\mathbf{q}) \dot{\mathbf{u}} - \mathbf{h}(\mathbf{q}, \mathbf{u}, \boldsymbol{\tau}) - \sum_i \mathbf{J}_i^\top(\mathbf{q}) \mathbf{f}_{ext,i} = 0 \\ & \text{(2)} \quad \|\mathbf{q}\| \leq q_{max} \\ & \text{(3)} \quad \|\boldsymbol{\tau}\| \leq \tau_{max} \end{aligned} \quad (3.6)$$

where q_{max} and τ_{max} denote maximum joint movements and actuation torques, respectively. In the above optimization problem, (1), (2), and (3) enforce dynamics agreement, kinematics restrictions, and actuation saturations, respectively.

CHAPTER 3. CONTACT MODELLING

Subsequently, a time-stepping methodology facilitates the integration of system dynamics across a time interval Δt while internally addressing the resolution of contact forces. We employ the shooting method to find the optimal joint positions \mathbf{u}_{ref} for minimizing $\frac{1}{2}\mathbf{f}_{ext}^\top \mathbf{G} \mathbf{f}_{ext} + \mathbf{f}_{ext}^\top \mathbf{c}$, ensuring that the generalized contact forces \mathbf{f}_{ext} are orthogonal to gap functions and their derivatives.

Chapter 4

Results

We performed numerical dynamics integration of COBRA and a box interactions on flat ground. In Fig. 4.1, snapshots illustrating simulated forward box push using C-, S-, J-shaped lateral rolling, and sidewinding gait are presented. In these simulations, the goal is to move the box on the flat ground towards a specified point, and corresponding suitable joint commands are derived. The J-shaped lateral rolling gait is asymmetrical and can be mirrored to execute control on the direction in which the object is moved. The composite Fig. 4.2 illustrates the contact points and unilateral ground reaction forces during (a) C-shaped gait, (b) S-shaped gait, (c) J-shaped gait, and (d) sidewinding gait, executed by the high-fidelity COBRA model simulated in the MATLAB environment. The contact forces encompass tangential forces ($f_{T,i}$) and normal forces ($f_{N,i}$), where Lx denotes Link number x on the robot, numbered from 1 to 10 starting from the head.

Fig 4.3 shows the torques for the central yawing and pitching joints. The torque plots look identical across the robot for the yawing and pitching joints each with a phase difference. We get these values from our Simscape actuator model, since we do not have the capability of achieving this from hardware yet. Using these torques we can further analyse the efficiency of each of these rolling gaits.

Figures 4.4 and 4.5 compare the efficiency of the four gaits in performing the prescribed task of moving the box. Figure 4.4 plots the work done internally by the robot for locomotion against the work done by the robot on the box. The joint torques τ for the gaits are shown in Fig. 4.3.

More efficient gaits would need less work in locomotion to do more work on the box. In this respect, the S and J shape lateral rolling gaits perform more efficiently than other gaits, with Sidewinding doing the most work on the box, but consuming the most energy to do it. This is corroborated by the plot of instantaneous power for the robot for locomotion in Fig. 4.5 that show

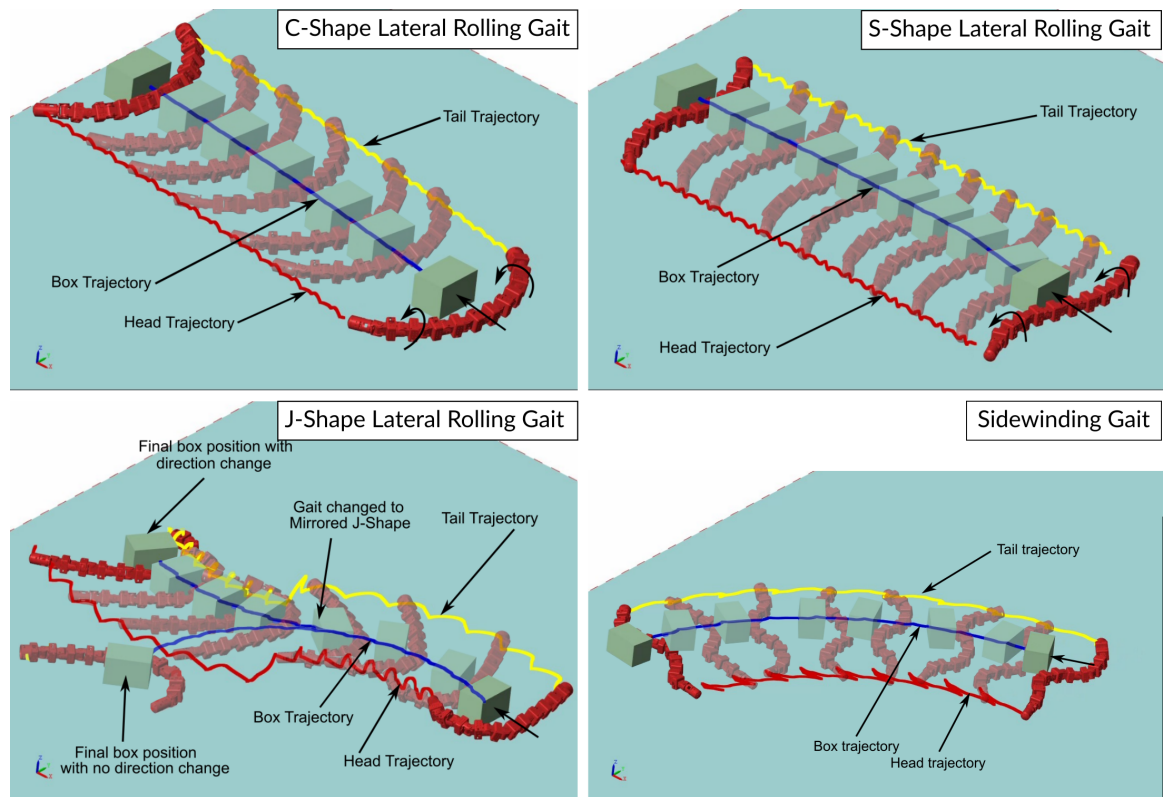


Figure 4.1: Snapshots depicting simulated forward box push utilizing various gaits executed in Matlab. The J-shape gait is an asymmetric variation of the C-gait, which allows changing the direction of movement of the box by mirroring the gait.

CHAPTER 4. RESULTS

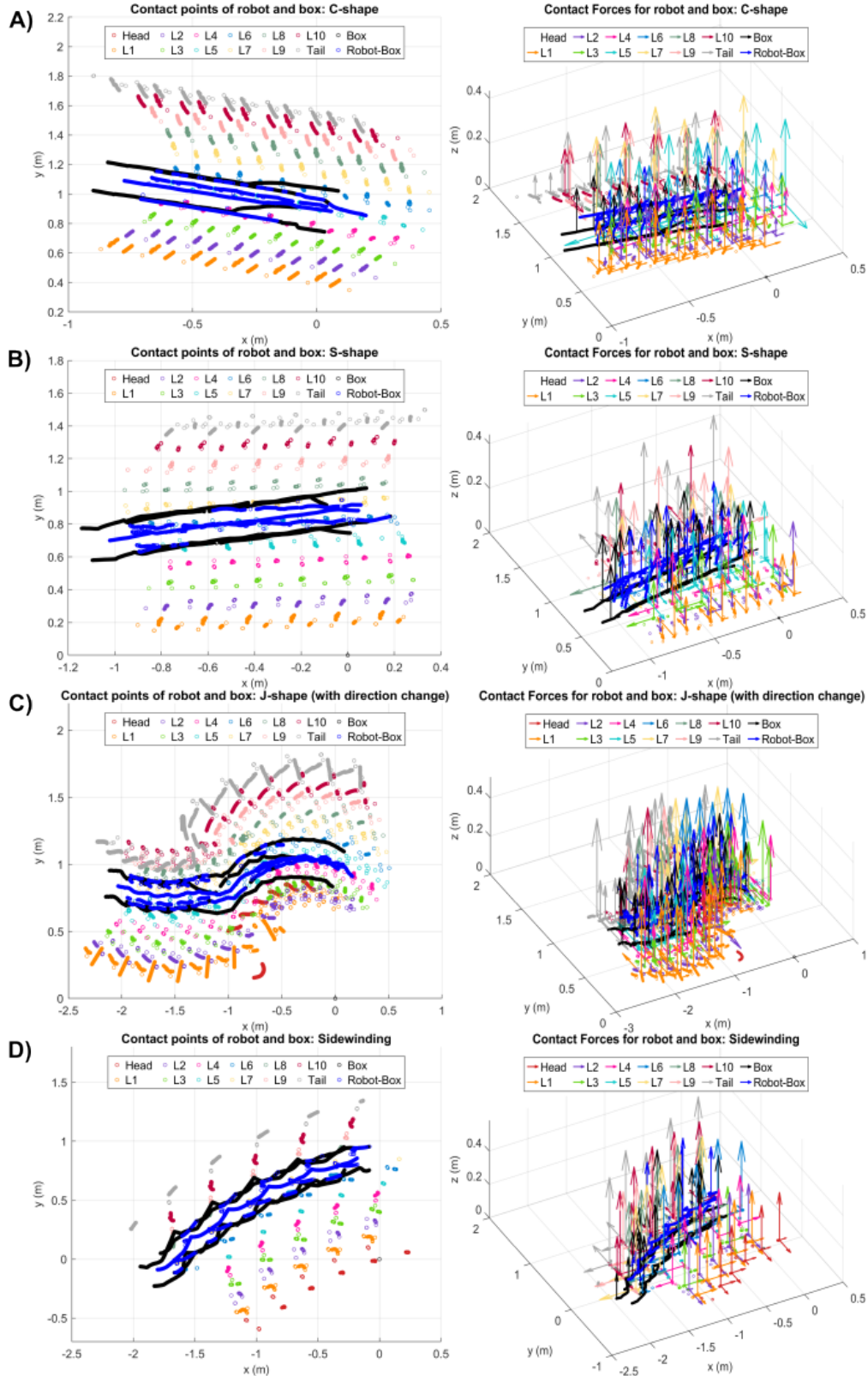


Figure 4.2: This image depicts the contact point and unilateral ground reaction forces during (A): C-shaped gaits, (B) S-Shaped Gait, (C) J-Shaped Gait, (D) Sidewinding gait, performed by the high-fidelity COBRA model simulated in the MATLAB environment. The contact forces consist

CHAPTER 4. RESULTS

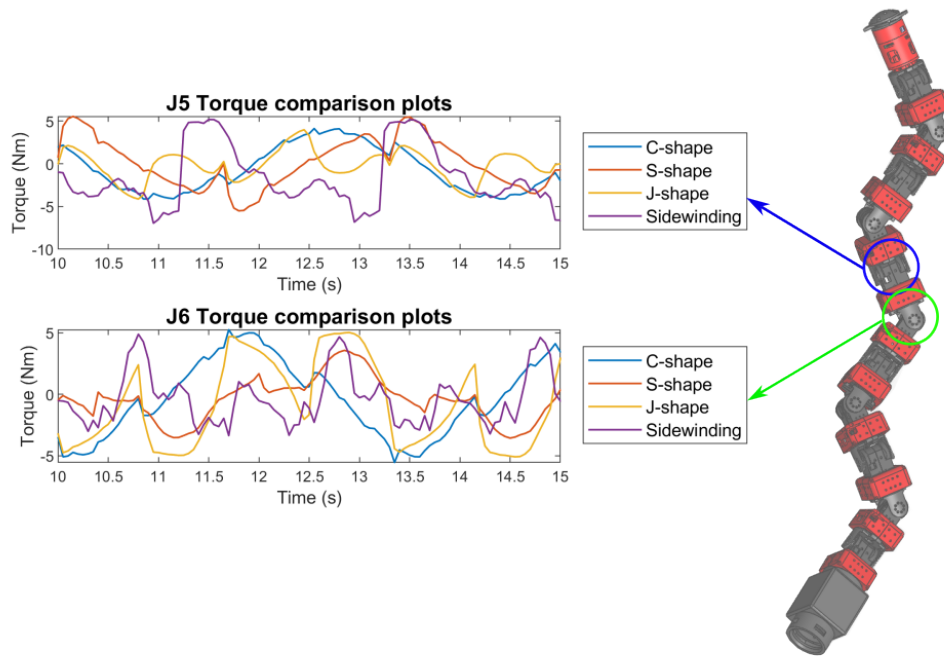


Figure 4.3: Depicts the torque profile for the central yawing (J6) and pitching (J5) joints for each gait. Other joints show similar profiles offset by a phase angle based on the executed gait.

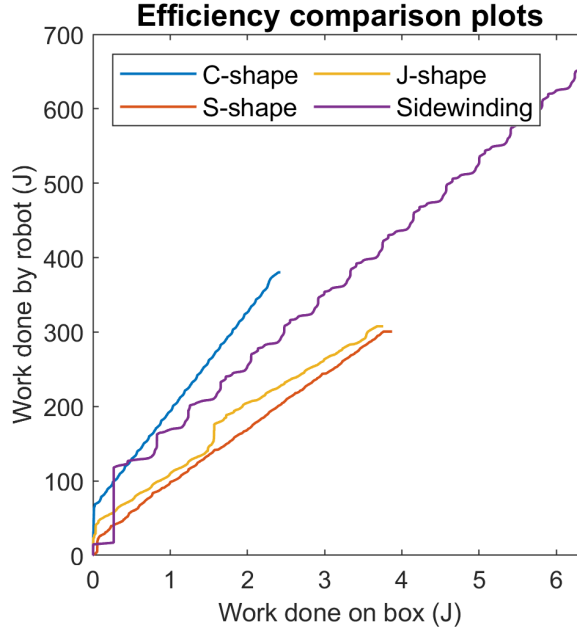


Figure 4.4: Depicts the efficiency of each gait based on the total work done by the robot for locomotion against total work done on the box. Larger slope indicates a less efficient gait as more work is done on locomotion in return for smaller work done on the box.

the large peaks in instantaneous power from sidewinding, as compared to the more steady power consumption by other gaits. This results in a slower but more energy efficient loco-manipulation. Figure 4.6 shows the relative distance moved by the box as a result of each gait operating for the same amount of time.

We implemented the same gaits on hardware, as shown in fig 4.7. We have our custom-made Optitrack attachments which gives us data for the head, tail and the box locations for our entire gait. We use this inform to make comparison between the head, tail and box trajectories from simscape and the same trajectories obtained from optitrack, which can be seen in fig 4.8. From this graphs we can conclude that we can accurately replicate the results from our simscape model on our hardware.

Once we achieved accurate hardware results, we demonstrate the object manipulation with COBRA by implementing the obtained desired trajectories in an open-loop fashion to show the effectiveness of our approach in preparation for the hardware implementation of the presented optimization model in closed-loop fashion.

Figure 4.9 shows COBRA lifting an object from the ground and placing it on a raised

CHAPTER 4. RESULTS

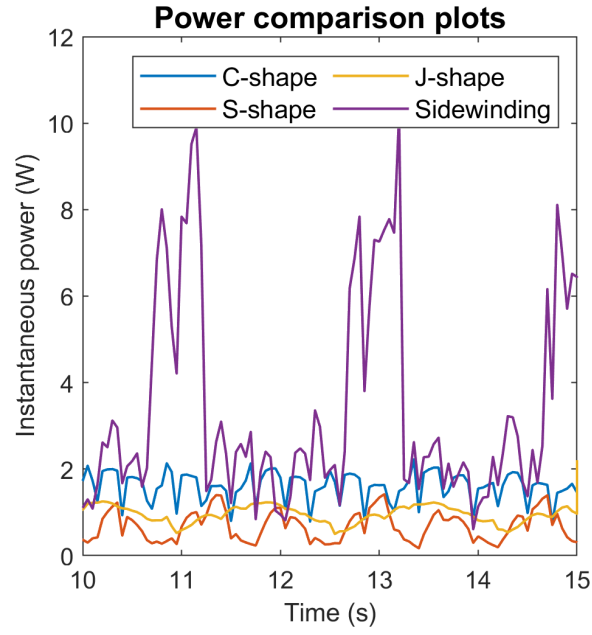


Figure 4.5: Shows the instantaneous power consumption by the robot to execute locomotion for each of the considered gaits.

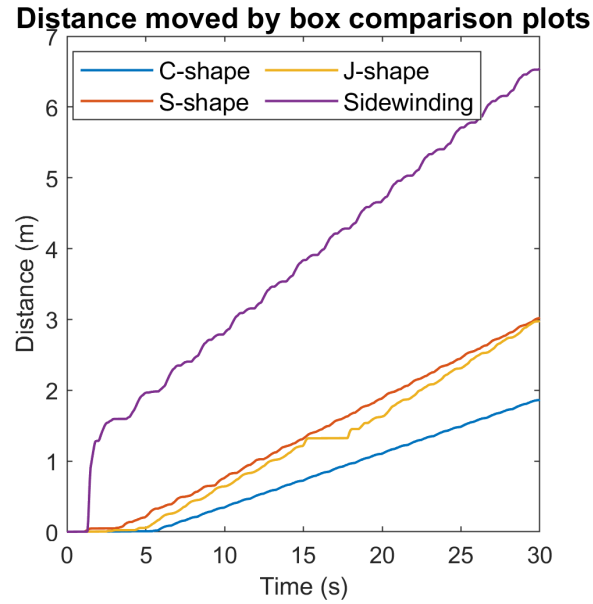


Figure 4.6: Depicts the total distance the robot moves the box for each gait in the same amount of time.

CHAPTER 4. RESULTS

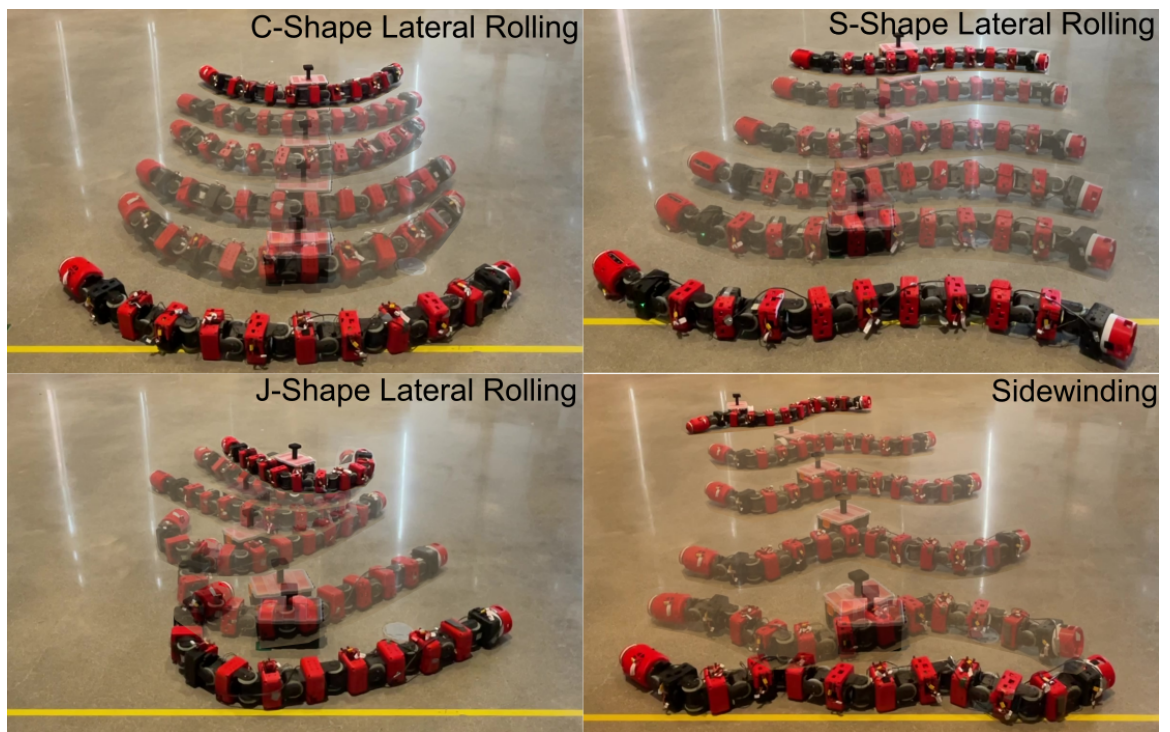


Figure 4.7: Shows the hardware implementation of the lateral rolling gaits performed in Simscape model

CHAPTER 4. RESULTS

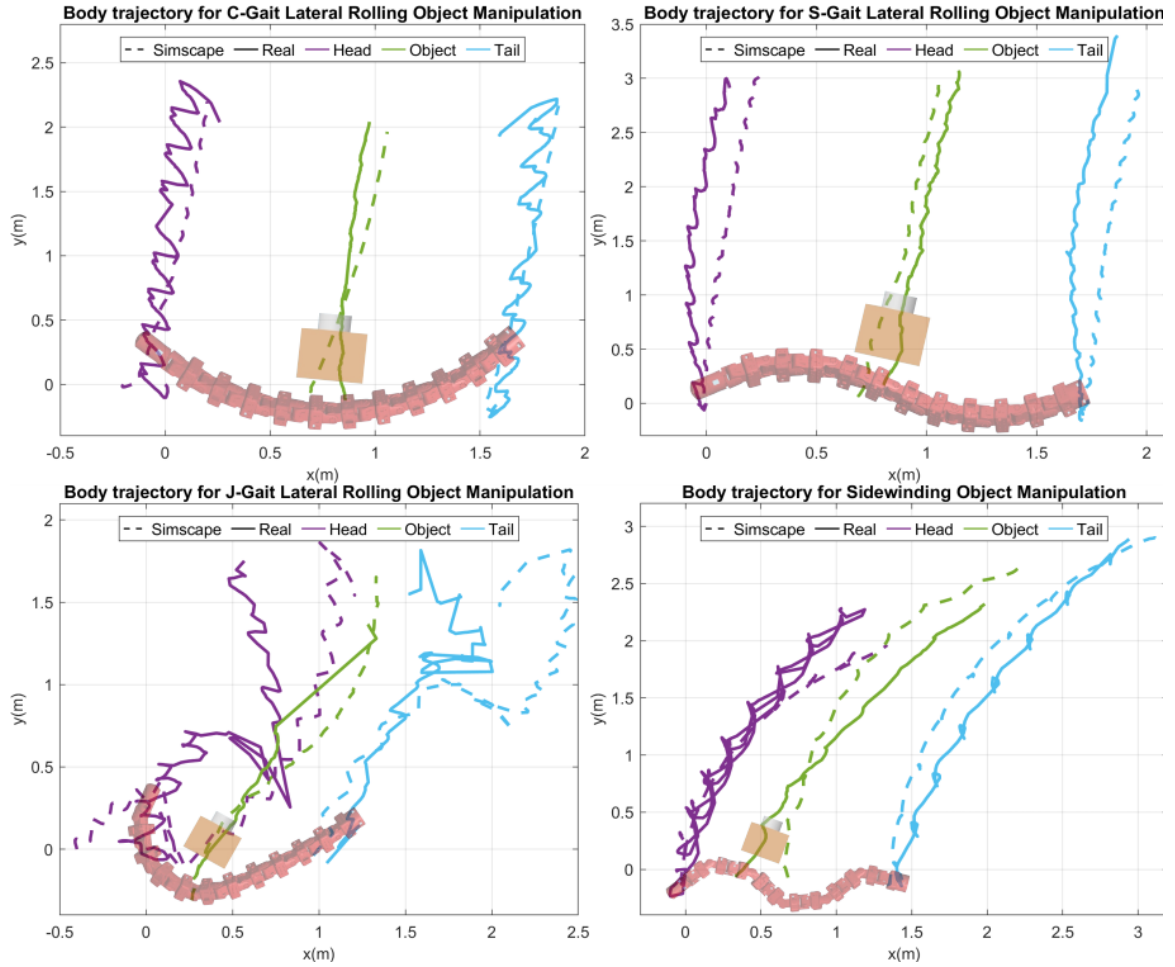


Figure 4.8: Shows comparison between simscape and real robot of robot and box for the various lateral rolling gaits on flat ground shown from top view

CHAPTER 4. RESULTS

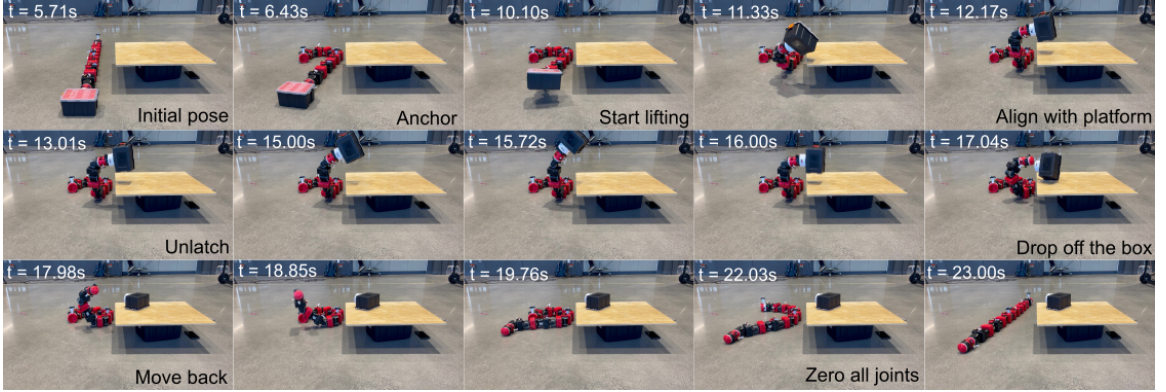


Figure 4.9: Snapshots of COBRA lifting a box and placing it on a raised platform.

platform of height 0.3m. The robot starts with the object docked to the head module using the docking module shown in Fig. 2.4. It curls the tail to increase the region of support, allowing it to stay balanced while lifting the box up to a height of 0.4m from the ground. Once it has moved the box over the platform, it unlatches from the object and shakes its head to dislodge it and deposit it on the platform. Fig. 4.13 shows the box trajectory and robot contact forces for the entire trajectory.

In Fig. 4.10 and Fig. 4.11, first in simulation, then in experiment, the robot starts on the ground with the object on the raised platform. The robot is able to, once again, curl its tail and lift the head to align itself with the docking module on the object. With some manipulation to allow the box to align to the latch, the robot can latch onto the box and place it in front of the body. From this position, COBRA can use its lateral rolling gait to move the object to a desired location.

Fig. 4.12 shows COBRA picking up the box from a raised platform, placing it in front of the body and moving the box to the top of a ramp. Fig. 4.14 shows the box trajectory and contact forces for loco-manipulation up an inclined ramp.

CHAPTER 4. RESULTS

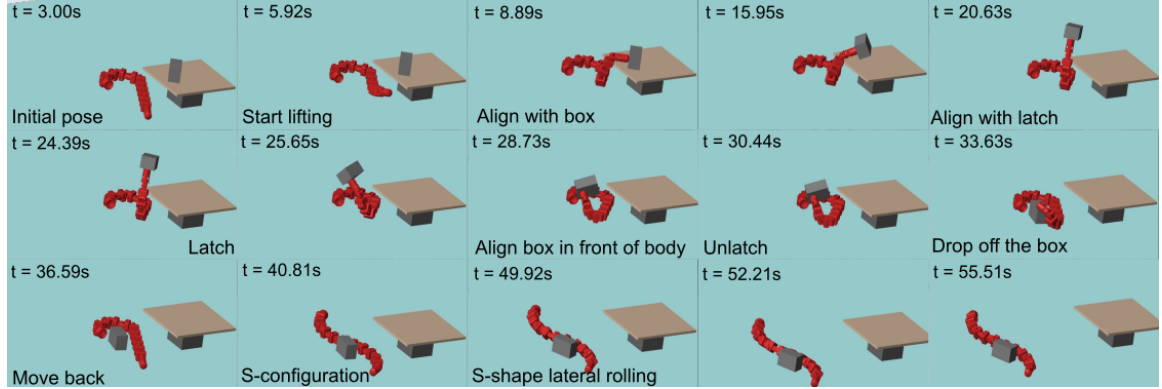


Figure 4.10: Snapshots depict simulation of COBRA lifting a box from a raised platform, placing it on the flat ground, and translating the box to a new location through continuous body-object interactions during slithering motions.

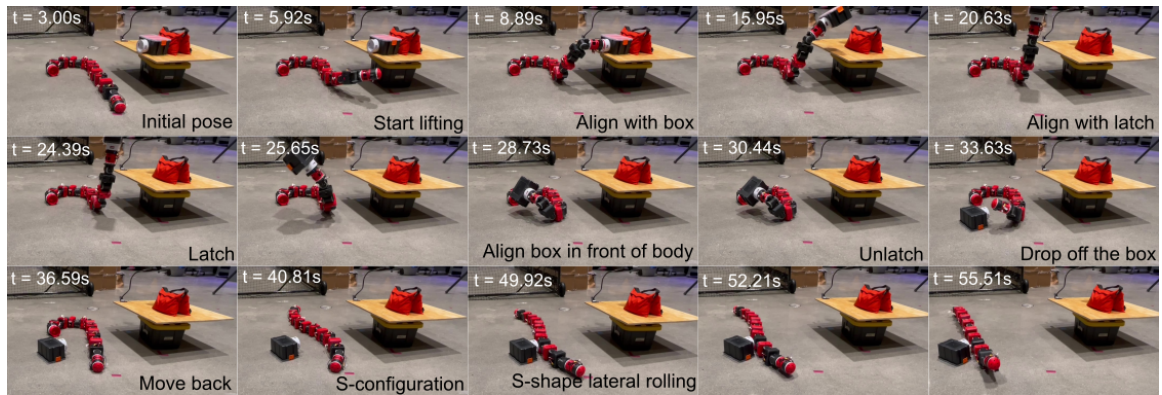


Figure 4.11: Snapshots depict COBRA lifting a box from a raised platform, placing it on the flat ground, and translating the box to a new location through continuous body-object interactions during slithering motions.

CHAPTER 4. RESULTS

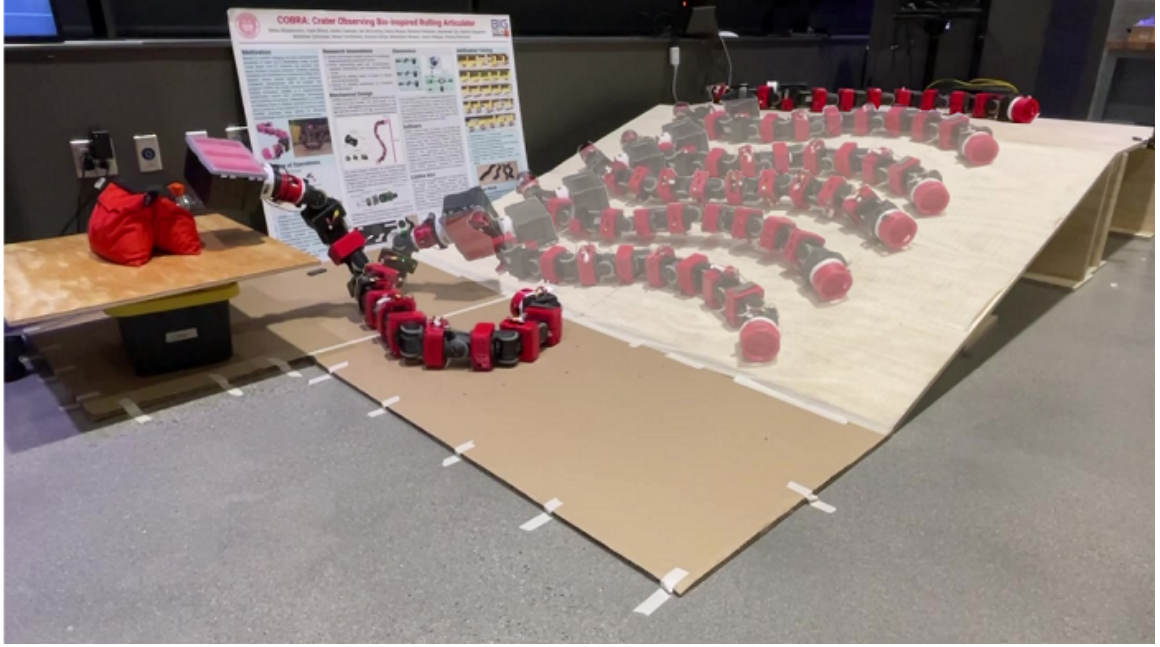


Figure 4.12: Snapshots capture COBRA lifting a box from a raised platform, setting it down on the ground, and ascending a ramp by continually pushing the box while lateral rolling.

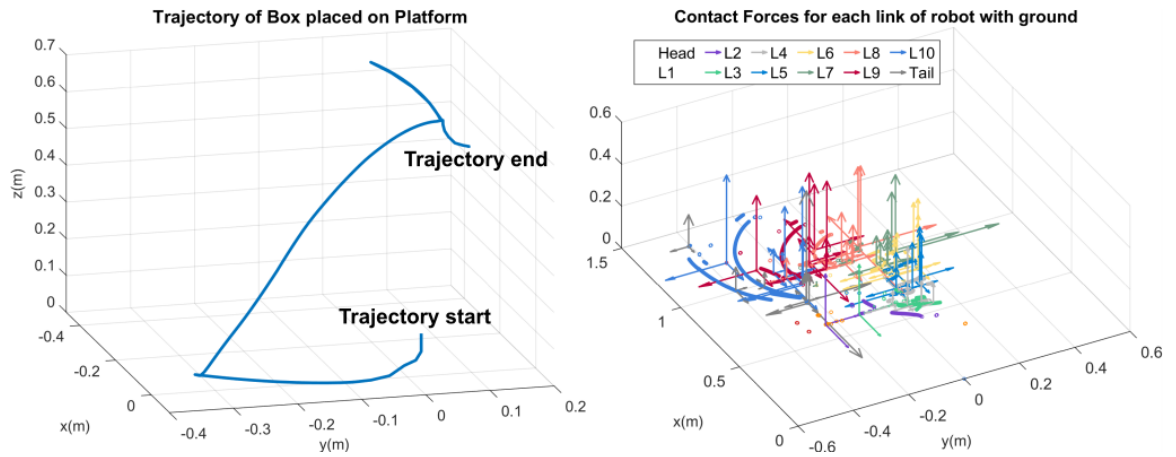


Figure 4.13: (Left) Shows the trajectory of the box while being lifted from ground and placed on a raised platform. (Right) Shows the contact forces between the robot and ground during the entire trajectory

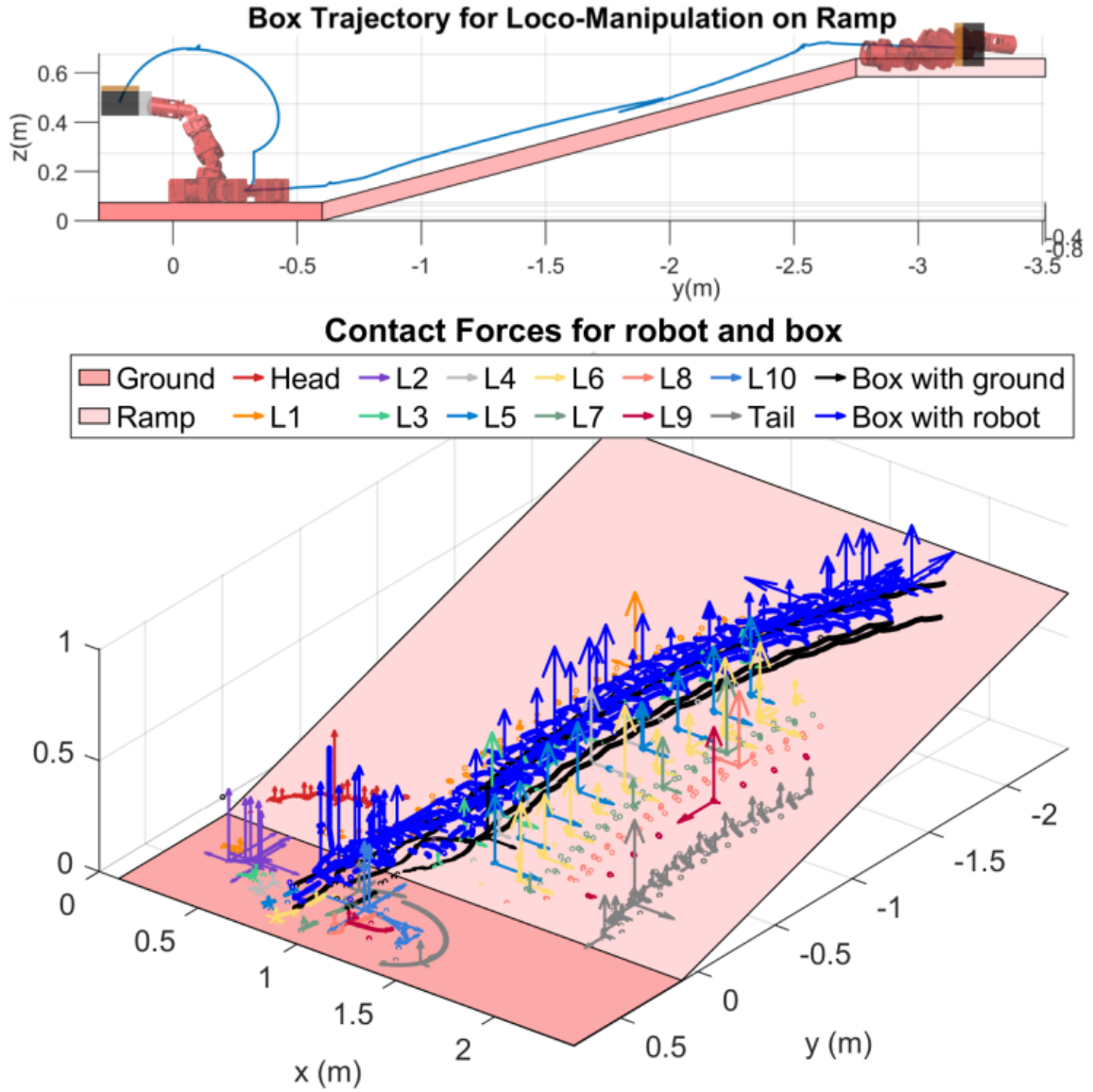


Figure 4.14: (Top) Shows the box trajectory during picking from platform, placing on ground and manipulating to the top of the ramp. (Bottom) Contact forces for the robot and box during picking the box from a raised platform, placing on the ground, and manipulation using s-lateral rolling gait up a ramp.

Chapter 5

Conclusion

Within the scope of this thesis, I have undertaken the development of finely-tuned open-loop gaits tailored specifically for achieving loco-manipulation capabilities on the COBRA platform. With its 11 actuated joints and integrated sensing and computation capabilities, COBRA emerges as a formidable platform, facilitating meticulous modeling for the manipulation of objects across flat surfaces. I worked on developing various gaits, each meticulously crafted to realize planar loco-manipulation objectives. Comparative analysis of these gaits, using metrics such as efficiency and instantaneous power plots, served as the cornerstone for determining the optimal gait patterns. Subsequently, I delved into the realm of more complex manipulation tasks, including the lifting a box from ground-level and placing it onto elevated platforms. Having successfully achieved proficiency in these tasks, I embarked upon the integration of these skills with planar loco-manipulation techniques. Leveraging the capabilities of COBRA, I demonstrated maneuvers wherein the robot adeptly lifted a box from a raised platform, positioned it in front of itself, and then navigated to a predetermined location on level ground. Additionally, I replicated the same level of loco-manipulation proficiency when navigating up an inclined ramp. Furthermore, collaboration with Professor Alireza Ramezani and Adarsh Salagame, yielded significant strides in the development of a contact-rich optimization-based control methodology. This innovative approach holds promise for the creation of a closed-loop controller, offering enhanced precision and adaptability in executing manipulation tasks. In summation, this thesis encapsulates a multifaceted journey encompassing the refinement and application of locomotive manipulation techniques on the COBRA platform. The culmination of these efforts not only advances our understanding of robotic manipulation but also lays the groundwork for future developments in closed-loop control strategies.

5.1 Challenges in existing setup

Following our work on achieving loco-manipulation tasks with COBRA, I encountered several immediate challenges. Firstly, our current Simulink setup lacks a friction model that accurately mirrors real-world friction forces. Developing a controller that incorporates such a precise friction model is imperative to address this issue. Additionally, we observed compliance in joints due to 3D printed components and servo backlash. Compensation for servo backlash can be achieved through encoder data. However, we currently lack an estimator for 3D print compliance. Furthermore, with our current open-loop gaits, we face limitations in planning locomotion for the snake to accomplish tasks for which a gait hasn't been predefined. Lastly, the absence of any perception capabilities on the robot necessitates the predefinition of the locations for the box, platform, and ramp to design our open-loop gaits.

5.2 Future Scope

Examining the challenges outlined in the previous section, there are viable strategies to tackle them. Firstly, leveraging our established mathematical model, we can proceed to develop a closed-loop controller. Within this controller framework, we can incorporate an estimator designed to accommodate joint compliance, thus enhancing overall control precision. Moreover, an avenue for improvement lies in the integration of sensory technologies. This includes the utilization of IMUs (Inertial Measurement Units) and force or tactile sensors to augment our feedback capabilities. By integrating these sensors, we gain valuable insights into the robot's interactions with its environment, facilitating more nuanced control and maneuvering. Furthermore, the incorporation of a RealSense camera system presents an opportunity to enhance perception capabilities. The RealSense camera can provide depth maps and enable object tracking within the operational environment. This additional sensory input empowers the robot with a more comprehensive understanding of its surroundings, thereby facilitating online and real-time path planning and re-planning based on the dynamic feedback received from these sensors.

Bibliography

- [1] Khalil Alipour and S. Ali A. Moosavian. “Dynamically stable motion planning of wheeled robots for heavy object manipulation”. In: *Advanced Robotics* (Apr. 2015).
- [2] Janis Arents and Modris Greitans. “Smart Industrial Robot Control Trends, Challenges and Opportunities within Manufacturing”. In: *Applied Sciences* 12.2 (Jan. 2022), p. 937. DOI: 10.3390/app12020937.
- [3] Pinhas Ben-Tzvi, Andrew A. Goldenberg, and Jean W. Zu. “Design, simulations and optimization of a tracked mobile robot manipulator with hybrid locomotion and manipulation capabilities”. In: *2008 IEEE International Conference on Robotics and Automation*. May 2008, pp. 2307–2312. DOI: 10.1109/ROBOT.2008.4543558.
- [4] Aude Billard and Danica Kragic. “Trends and challenges in robot manipulation”. In: *Science* 364.6446 (June 2019), eaat8414. DOI: 10.1126/science.aat8414.
- [5] Karen Bodie, C. Dario Bellicoso, and Marco Hutter. “ANYpulator: Design and control of a safe robotic arm”. In: *2016 IEEE/RSJ International Conference on Intelligent Robots and Systems (IROS)*. Daejeon, South Korea: IEEE, Oct. 2016, pp. 1119–1125. DOI: 10.1109/IROS.2016.7759189.
- [6] *Boston Dynamics Expands Global Sales of Spot® Robot*. en-US. URL: <https://bostondynamics.com/news/boston-dynamics-expands-global-sales-of-spot-robot/> (visited on 04/12/2024).
- [7] J.W. Burdick, J. Radford, and G.S. Chirikjian. “A ‘sidewinding’ locomotion gait for hyper-redundant robots”. In: *Advanced Robotics* 9.3 (Jan. 1994), pp. 195–216. DOI: 10.1163/156855395X00166.

BIBLIOGRAPHY

- [8] Jan Carius et al. “Trajectory Optimization With Implicit Hard Contacts”. In: *IEEE Robotics and Automation Letters* 3.4 (Oct. 2018), pp. 3316–3323. DOI: 10.1109/LRA.2018.2852785.
- [9] Ravinesh Chand et al. “Vertically Sliding Revolute Robotic Arm intended for automated Pick-and-Place Industrial applications”. In: *2022 IEEE Asia-Pacific Conference on Computer Science and Data Engineering (CSDE)*. Gold Coast, Australia: IEEE, Dec. 2022, pp. 1–5. DOI: 10.1109/CSDE56538.2022.10089325.
- [10] Li Chen et al. “Studies on lateral rolling locomotion of a snake robot”. In: *IEEE International Conference on Robotics and Automation, 2004. Proceedings. ICRA '04. 2004*. Vol. 5. Apr. 2004, pp. 5070–5074. DOI: 10.1109/ROBOT.2004.1302521.
- [11] Tiffany L Chen et al. “Robots for Humanity: A Case Study in Assistive Mobile Manipulation”. In: ().
- [12] Pravin Dangol and Alireza Ramezani. “Thruster-assisted legged robot control (Conference Presentation)”. In: *Unmanned Systems Technology XXII*. Vol. 11425. International Society for Optics and Photonics, Apr. 2020, p. 1142507. DOI: 10.1117/12.2558284.
- [13] Pravin Dangol, Eric Sihite, and Alireza Ramezani. “Control of Thruster-Assisted, Bipedal Legged Locomotion of the Harpy Robot”. In: *Frontiers in Robotics and AI* 8 (Dec. 2021). DOI: 10.3389/frobt.2021.770514.
- [14] Yanran Ding, Abhishek Pandala, and Hae-Won Park. “Real-time Model Predictive Control for Versatile Dynamic Motions in Quadrupedal Robots”. In: *2019 International Conference on Robotics and Automation (ICRA)*. May 2019, pp. 8484–8490. DOI: 10.1109/ICRA.2019.8793669.
- [15] Greg Droge and Magnus Egerstedt. “Optimal decentralized gait transitions for snake robots”. In: *2012 IEEE International Conference on Robotics and Automation*. May 2012, pp. 317–322. DOI: 10.1109/ICRA.2012.6224721.
- [16] Alessandra Duz et al. *Robotic Autonomous Loco-Manipulation For Logistics In Industrial Plants*. Oct. 2022. DOI: 10.5281/zenodo.7531364.
- [17] Íñigo Elguea-Aguinaco et al. “A review on reinforcement learning for contact-rich robotic manipulation tasks”. In: *Robotics and Computer-Integrated Manufacturing* 81 (June 2023), p. 102517. DOI: 10.1016/j.rcim.2022.102517.

BIBLIOGRAPHY

- [18] Belal A. Elsayed et al. “Mobile Manipulation Using a Snake Robot in a Helical Gait”. In: *IEEE/ASME Transactions on Mechatronics* 27.5 (Oct. 2022), pp. 2600–2611. DOI: 10.1109/TMECH.2021.3114168.
- [19] *Feedback Control Design for MARLO, a 3D-Bipedal Robot*. URL: <https://deepblue.lib.umich.edu/handle/2027.42/102339> (visited on 05/09/2020).
- [20] Henrique Ferrolho et al. “Optimizing Dynamic Trajectories for Robustness to Disturbances Using Polytopic Projections”. In: *2020 IEEE/RSJ International Conference on Intelligent Robots and Systems (IROS)*. Las Vegas, NV, USA: IEEE, Oct. 2020, pp. 7477–7484. DOI: 10.1109/IROS45743.2020.9341788.
- [21] Rory Flemmer and Claire Flemmer. *A Humanoid Robot for Research into Kicking Rugby Balls*. Jan. 2014. DOI: 10.13140/RG.2.1.2755.3122.
- [22] Qiyuan Fu and Chen Li. “Robotic modelling of snake traversing large, smooth obstacles reveals stability benefits of body compliance”. In: *Royal Society Open Science* 7.2 (Feb. 2020), p. 191192. DOI: 10.1098/rsos.191192.
- [23] N. Giri and I. Walker. “Continuum robots and underactuated grasping”. In: *Mechanical Sciences* 2.1 (Feb. 2011), pp. 51–58. DOI: 10.5194/ms-2-51-2011.
- [24] Yifeng Gong et al. “Legged robots for object manipulation: A review”. In: *Frontiers in Mechanical Engineering* 9 (Apr. 2023). DOI: 10.3389/fmech.2023.1142421.
- [25] Nicolas Guéguen et al. “Hey Buddy, Can You Give Me 37 s of Your Time? Extension of the Pique Technique to a Non-monetary Solicitation and Test of Justification for Compliance”. In: *Current Psychology* 35.4 (Dec. 2016), pp. 583–586. DOI: 10.1007/s12144-015-9324-z.
- [26] Sangchul Han et al. “Snake Robot Gripper Module for Search and Rescue in Narrow Spaces”. In: *IEEE Robotics and Automation Letters* 7.2 (Apr. 2022), pp. 1667–1673. DOI: 10.1109/LRA.2022.3140812.
- [27] M.W. Hannan and I.D. Walker. “The ‘elephant trunk’ manipulator, design and implementation”. In: *2001 IEEE/ASME International Conference on Advanced Intelligent Mechatronics. Proceedings (Cat. No.01TH8556)*. Vol. 1. July 2001, 14–19 vol.1. DOI: 10.1109/AIM.2001.936423.
- [28] G Heppner et al. “LAUROPE - SIX LEGGED WALKING ROBOT FOR PLANETARY EXPLORATION PARTICIPATING IN THE SPACEBOT CUP”. In: ().

BIBLIOGRAPHY

- [29] S. Hirose et al. “Quadruped Walking Robot Centered Demining System - Development of TITAN-IX and its Operation-”. In: *Proceedings of the 2005 IEEE International Conference on Robotics and Automation*. Barcelona, Spain: IEEE, 2005, pp. 1284–1290. DOI: 10.1109/ROBOT.2005.1570292.
- [30] Shigeo Hirose and Hiroya Yamada. “Snake-like robots [Tutorial]”. In: *IEEE Robotics & Automation Magazine* 16.1 (Mar. 2009), pp. 88–98. DOI: 10.1109/MRA.2009.932130.
- [31] Jane Holland et al. “Service Robots in the Healthcare Sector”. In: *Robotics* 10.1 (Mar. 2021), p. 47. DOI: 10.3390/robotics10010047.
- [32] Kenji Inoue, Kanjiro Ooe, and Suwoong Lee. “Pushing methods for working six-legged robots capable of locomotion and manipulation in three modes”. In: *2010 IEEE International Conference on Robotics and Automation*. Anchorage, AK: IEEE, May 2010, pp. 4742–4748. DOI: 10.1109/ROBOT.2010.5509220.
- [33] A.E Jimenez-Cano et al. “Aerial manipulator for structure inspection by contact from the underside”. In: *2015 IEEE/RSJ International Conference on Intelligent Robots and Systems (IROS)*. Hamburg, Germany: IEEE, Sept. 2015, pp. 1879–1884. DOI: 10.1109/IROS.2015.7353623.
- [34] Muhammad Aqib Khan. “Design and control of a robotic system based on mobile robots and manipulator arms for picking in logistics warehouses”. In: ().
- [35] Byeongjun Kim et al. “Globally Defined Dynamic Modelling and Geometric Tracking Controller Design for Aerial Manipulator”. In: *2023 IEEE International Conference on Robotics and Automation (ICRA)*. May 2023, pp. 5386–5392. DOI: 10.1109/ICRA48891.2023.10160860.
- [36] Sandeep Ameet Kumar et al. “Linear manipulator: Motion control of an n-link robotic arm mounted on a mobile slider”. In: *Heliyon* 9.1 (Jan. 2023), e12867. DOI: 10.1016/j.heliyon.2023.e12867.
- [37] Puneet Kumar Singh and C. Murali Krishna. “Continuum Arm Robotic Manipulator: A Review”. In: *Universal Journal of Mechanical Engineering* 2.6 (June 2014), pp. 193–198. DOI: 10.13189/ujme.2014.020603.

BIBLIOGRAPHY

- [38] Kaier Liang et al. “Rough-Terrain Locomotion and Unilateral Contact Force Regulations With a Multi-Modal Legged Robot”. In: *2021 American Control Conference (ACC)*. New Orleans, LA, USA: IEEE, May 2021, pp. 1762–1769. DOI: 10.23919/ACC50511.2021.9483189.
- [39] Pål Liljebäck, Øyvind Stavdahl, and Kristin Y. Pettersen. “MODULAR PNEUMATIC SNAKE ROBOT 3D MODELLING, IMPLEMENTATION AND CONTROL”. In: *IFAC Proceedings Volumes*. 16th IFAC World Congress 38.1 (Jan. 2005), pp. 19–24. DOI: 10.3182/20050703-6-CZ-1902.01274.
- [40] Maria S. Lopes et al. “A Review on Quadruped Manipulators”. In: *Progress in Artificial Intelligence*. Cham: Springer Nature Switzerland, 2023, pp. 199–211. DOI: 10.1007/978-3-031-49008-8_16.
- [41] Shugen Ma et al. “Analysis of creeping locomotion of a snake robot on a slope”. In: *2003 IEEE International Conference on Robotics and Automation (Cat. No.03CH37422)*. Vol. 2. Sept. 2003, 2073–2078 vol.2. DOI: 10.1109/ROBOT.2003.1241899.
- [42] *MABEL: the world’s fastest knee-equipped bipedal robot*. en-US. Section: Robotics. Aug. 2011. URL: <https://newatlas.com/mabel-the-running-robot/19558/> (visited on 04/01/2024).
- [43] Xiangdong Meng, Yuqing He, and Jianda Han. “Survey on Aerial Manipulator: System, Modeling, and Control”. In: *Robotica* 38.7 (July 2020), pp. 1288–1317. DOI: 10.1017/S0263574719001450.
- [44] Michael E. Moran. “Evolution of robotic arms”. In: *Journal of Robotic Surgery* 1.2 (July 2007), pp. 103–111. DOI: 10.1007/s11701-006-0002-x.
- [45] H. Ohno and S. Hirose. “Design of slim slime robot and its gait of locomotion”. In: *Proceedings 2001 IEEE/RSJ International Conference on Intelligent Robots and Systems. Expanding the Societal Role of Robotics in the the Next Millennium (Cat. No.01CH37180)*. Vol. 2. Oct. 2001, 707–715 vol.2. DOI: 10.1109/IROS.2001.976252.
- [46] Arthur C. B. de Oliveira and Alireza Ramezani. “Thruster-assisted Center Manifold Shaping in Bipedal Legged Locomotion”. In: *2020 IEEE/ASME International Conference on Advanced Intelligent Mechatronics (AIM)*. July 2020, pp. 508–513. DOI: 10.1109/AIM43001.2020.9158967.

BIBLIOGRAPHY

- [47] Evangelos Papadopoulos et al. “Robotic Manipulation and Capture in Space: A Survey”. In: *Frontiers in Robotics and AI* 8 (July 2021). DOI: 10.3389/frobt.2021.686723.
- [48] Hae-Won Park, Alireza Ramezani, and J. W. Grizzle. “A Finite-State Machine for Accommodating Unexpected Large Ground-Height Variations in Bipedal Robot Walking”. In: *IEEE Transactions on Robotics* 29.2 (Apr. 2013), pp. 331–345. DOI: 10.1109/TRO.2012.2230992.
- [49] Maria Pozzi et al. “Modeling and Simulation of Robotic Grasping in Simulink Through Simscape Multibody”. In: *Frontiers in Robotics and AI* 9 (May 2022). DOI: 10.3389/frobt.2022.873558.
- [50] Larona Pitso Ramalepa and Rodrigo S. Jamisola. “A Review on Cooperative Robotic Arms with Mobile or Drones Bases”. In: *International Journal of Automation and Computing* 18.4 (Aug. 2021), pp. 536–555. DOI: 10.1007/s11633-021-1299-7.
- [51] Alireza Ramezani. “Towards biomimicry of a bat-style perching maneuver on structures: the manipulation of inertial dynamics”. In: *2020 IEEE International Conference on Robotics and Automation (ICRA)*. Paris, France: IEEE, May 2020, pp. 7015–7021. DOI: 10.1109/ICRA40945.2020.9197376.
- [52] Alireza Ramezani, Soon-Jo Chung, and Seth Hutchinson. “A biomimetic robotic platform to study flight specializations of bats”. In: *Science Robotics* 2.3 (Feb. 2017), eaal2505. DOI: 10.1126/scirobotics.aal2505.
- [53] Alireza Ramezani and J.w. Grizzle. “Atrias 2.0, a new 3d bipedal robotic walker and runner”. In: *Adaptive Mobile Robotics*. WORLD SCIENTIFIC, May 2012, pp. 467–474. DOI: 10.1142/9789814415958_0060.
- [54] Alireza Ramezani et al. “Bat Bot (B2), a biologically inspired flying machine”. In: *2016 IEEE International Conference on Robotics and Automation (ICRA)*. Stockholm, Sweden: IEEE, May 2016, pp. 3219–3226. DOI: 10.1109/ICRA.2016.7487491.
- [55] Alireza Ramezani et al. “Describing Robotic Bat Flight with Stable Periodic Orbits”. In: *Biomimetic and Biohybrid Systems*. Lecture Notes in Computer Science. Cham: Springer International Publishing, 2017, pp. 394–405. DOI: 10.1007/978-3-319-63537-8_33.

BIBLIOGRAPHY

- [56] Alireza Ramezani et al. “Generative Design of NU’s Husky Carbon, A Morpho-Functional, Legged Robot”. In: *2021 IEEE International Conference on Robotics and Automation (ICRA)*. May 2021, pp. 4040–4046. DOI: 10.1109/ICRA48506.2021.9561196.
- [57] Alireza Ramezani et al. “Lagrangian modeling and flight control of articulated-winged bat robot”. In: *2015 IEEE/RSJ International Conference on Intelligent Robots and Systems (IROS)*. Hamburg, Germany: IEEE, Sept. 2015, pp. 2867–2874. DOI: 10.1109/IROS.2015.7353772.
- [58] Alireza Ramezani et al. “Modeling and nonlinear flight controller synthesis of a bat-inspired micro aerial vehicle”. In: *AIAA Guidance, Navigation, and Control Conference*. American Institute of Aeronautics and Astronautics Inc, AIAA, Jan. 2016.
- [59] Alireza Ramezani et al. “Nonlinear Flight Controller Synthesis of a Bat-Inspired Micro Aerial Vehicle”. In: *AIAA Guidance, Navigation, and Control Conference*. American Institute of Aeronautics and Astronautics. DOI: 10.2514/6.2016-1376.
- [60] Alireza Ramezani et al. “Performance Analysis and Feedback Control of ATRIAS, A Three-Dimensional Bipedal Robot”. In: *Journal of Dynamic Systems, Measurement, and Control* 136.2 (Mar. 2014). DOI: 10.1115/1.4025693.
- [61] D.M. Rincon and J. Sotelo. “Ver-vite: dynamic and experimental analysis for inchwormlike biomimetic robots”. In: *IEEE Robotics & Automation Magazine* 10.4 (Dec. 2003), pp. 53–57. DOI: 10.1109/MRA.2003.1256298.
- [62] Divyanshu Sahu, Ramachandra Kodi, and Sartaj Singh. “Gait Analysis of Multi-Step Climbing Active Wheeled Snake Robot”. In: *2019 4th International Conference on Robotics and Automation Engineering (ICRAE)*. Nov. 2019, pp. 18–23. DOI: 10.1109/ICRAE48301.2019.9043828.
- [63] Adarsh Salagame et al. *A Letter on Progress Made on Husky Carbon: A Legged-Aerial, Multi-modal Platform*. arXiv:2207.12254 [cs, eess]. July 2022. URL: <http://arxiv.org/abs/2207.12254> (visited on 08/21/2023).
- [64] Adarsh Salagame et al. *How Strong a Kick Should be to Topple Northeastern’s Tumbling Robot?* arXiv:2311.14878 [cs, eess]. Nov. 2023. DOI: 10.48550/arXiv.2311.14878. URL: <http://arxiv.org/abs/2311.14878> (visited on 04/26/2024).

BIBLIOGRAPHY

- [65] Adarsh Salagame et al. *Quadrupedal Locomotion Control On Inclined Surfaces Using Collocation Method*. arXiv:2312.08621 [cs, eess]. Dec. 2023. DOI: 10.48550/arXiv.2312.08621. URL: <http://arxiv.org/abs/2312.08621> (visited on 04/26/2024).
- [66] Venkata Satya Durga Manohar Sahu, Padarbinda Samal, and Chinmoy Kumar Panigrahi. “Modelling, and control techniques of robotic manipulators: A review”. In: *Materials Today: Proceedings*. 3rd International Conference on Contemporary Advances in Mechanical Engineering 56 (Jan. 2022), pp. 2758–2766. DOI: 10.1016/j.matpr.2021.10.009.
- [67] Stephanie Schneider et al. *ReachBot: A Small Robot for Large Mobile Manipulation Tasks*. arXiv:2110.10829 [cs, eess]. Oct. 2021. URL: <http://arxiv.org/abs/2110.10829> (visited on 03/27/2024).
- [68] Y. Shan and Y. Koren. “Design and motion planning of a mechanical snake”. In: *IEEE Transactions on Systems, Man, and Cybernetics* 23.4 (Aug. 1993), pp. 1091–1100. DOI: 10.1109/21.247890.
- [69] Scott Shaw and Guillaume Sartoretti. “Keyframe-based CPG for Stable Gait Design and Online Transitions in Legged Robots”. In: *2022 IEEE 61st Conference on Decision and Control (CDC)*. Cancun, Mexico: IEEE, Dec. 2022, pp. 756–763. DOI: 10.1109/CDC51059.2022.9992457.
- [70] Anna Sibilska-Mroziewicz et al. “Framework for simulation-based control design evaluation for a snake robot as an example of a multibody robotic system”. In: *Multibody System Dynamics* 55.4 (Aug. 2022), pp. 375–397. DOI: 10.1007/s11044-022-09830-3.
- [71] E. Sihite, P. Kelly, and A. Ramezani. “Mechanism Design of a Bio-inspired Armwing Mechanism for Mimicking Bat Flapping Gait”. In: *arXiv:2010.04702 [cs]* (Oct. 2020).
- [72] Eric Sihite, Pravin Dangol, and Alireza Ramezani. “Optimization-free Ground Contact Force Constraint Satisfaction in Quadrupedal Locomotion”. In: *2021 60th IEEE Conference on Decision and Control (CDC)*. Dec. 2021, pp. 713–719. DOI: 10.1109/CDC45484.2021.9683155.
- [73] Eric Sihite, Pravin Dangol, and Alireza Ramezani. “Unilateral Ground Contact Force Regulations in Thruster-Assisted Legged Locomotion”. In: *2021 IEEE/ASME International Conference on Advanced Intelligent Mechatronics (AIM)*. July 2021, pp. 389–395. DOI: 10.1109/AIM46487.2021.9517648.

BIBLIOGRAPHY

- [74] Eric Sihite, Peter Kelly, and Alireza Ramezani. “Computational Structure Design of a Bio-Inspired Armwing Mechanism”. In: *IEEE Robotics and Automation Letters* 5.4 (Oct. 2020), pp. 5929–5936. DOI: 10.1109/LRA.2020.3010217.
- [75] Eric Sihite and Alireza Ramezani. “Enforcing nonholonomic constraints in Aerobat, a roosting flapping wing model”. In: *2020 59th IEEE Conference on Decision and Control (CDC)*. Dec. 2020, pp. 5321–5327. DOI: 10.1109/CDC42340.2020.9304158.
- [76] Eric Sihite and Alireza Ramezani. *Wake-Based Locomotion Gait Design for Aerobat*. arXiv:2212.05359 [cs, eess]. Dec. 2022. DOI: 10.48550/arXiv.2212.05359. URL: <http://arxiv.org/abs/2212.05359> (visited on 04/26/2024).
- [77] Eric Sihite, Alireza Ramezani, and Morteza Gharib. *Dynamic modeling of wing-assisted inclined running with a morphing multi-modal robot*. arXiv:2311.09963 [cs, eess]. Nov. 2023. DOI: 10.48550/arXiv.2311.09963. URL: <http://arxiv.org/abs/2311.09963> (visited on 04/26/2024).
- [78] Eric Sihite et al. “Actuation and Flight Control of High-DOF Dynamic Morphing Wing Flight by Shifting Structure Response”. In: *2023 62nd IEEE Conference on Decision and Control (CDC)*. Dec. 2023, pp. 8824–8829. DOI: 10.1109/CDC49753.2023.10383886.
- [79] Eric Sihite et al. “An Integrated Mechanical Intelligence and Control Approach Towards Flight Control of Aerobat”. In: *2021 American Control Conference (ACC)*. May 2021, pp. 84–91. DOI: 10.23919/ACC50511.2021.9482643.
- [80] Eric Sihite et al. *Bang-Bang Control Of A Tail-less Morphing Wing Flight*. arXiv:2205.06395 [cs, eess]. May 2022. DOI: 10.48550/arXiv.2205.06395. URL: <http://arxiv.org/abs/2205.06395> (visited on 04/26/2024).
- [81] Eric Sihite et al. *Demonstrating Autonomous 3D Path Planning on a Novel Scalable UGV-UAV Morphing Robot*. arXiv:2308.00235 [cs, eess]. July 2023. DOI: 10.48550/arXiv.2308.00235. URL: <http://arxiv.org/abs/2308.00235> (visited on 04/26/2024).
- [82] Eric Sihite et al. “Efficient Path Planning and Tracking for Multi-Modal Legged-Aerial Locomotion Using Integrated Probabilistic Road Maps (PRM) and Reference Governors (RG)”. In: *2022 IEEE 61st Conference on Decision and Control (CDC)*. Dec. 2022, pp. 764–770. DOI: 10.1109/CDC51059.2022.9992754.

BIBLIOGRAPHY

- [83] Eric Sihite et al. “Multi-Modal Mobility Morphobot (M4) with appendage repurposing for locomotion plasticity enhancement”. In: *Nature Communications* 14.1 (June 2023), p. 3323. DOI: 10.1038/s41467-023-39018-y.
- [84] Eric Sihite et al. *Orientation stabilization in a bioinspired bat-robot using integrated mechanical intelligence and control*. en. arXiv:2103.15943 [cs, eess]. Mar. 2021. URL: <http://arxiv.org/abs/2103.15943> (visited on 04/26/2024).
- [85] Eric Sihite et al. “Unsteady aerodynamic modeling of Aerobat using lifting line theory and Wagner’s function”. In: *2022 IEEE/RSJ International Conference on Intelligent Robots and Systems (IROS)*. Oct. 2022, pp. 10493–10500. DOI: 10.1109/IROS47612.2022.9982125.
- [86] Luka Skrinjar, Janko Slavič, and Miha Boltežar. “A review of continuous contact-force models in multibody dynamics”. In: *International Journal of Mechanical Sciences* 145 (Sept. 2018), pp. 171–187. DOI: 10.1016/j.ijmecsci.2018.07.010.
- [87] Jean-Pierre Sleiman, Farbod Farshidian, and Marco Hutter. “Versatile multicontact planning and control for legged loco-manipulation”. In: *Science Robotics* 8.81 (Aug. 2023), eadg5014. DOI: 10.1126/scirobotics.adg5014.
- [88] Jean-Pierre Sleiman et al. “Contact-Implicit Trajectory Optimization for Dynamic Object Manipulation”. In: *2019 IEEE/RSJ International Conference on Intelligent Robots and Systems (IROS)*. Nov. 2019, pp. 6814–6821. DOI: 10.1109/IROS40897.2019.8968194.
- [89] *Snake Robot Obstacle-Aided Locomotion: Modeling, Simulations, and Experiments — IEEE Journals & Magazine — IEEE Xplore*. URL: <https://ieeexplore.ieee.org/abstract/document/4456759> (visited on 03/22/2024).
- [90] Christian Studer. *Numerics of Unilateral Contacts and Friction: Modeling and Numerical Time Integration in Non-Smooth Dynamics*. en. Lecture Notes in Applied and Computational Mechanics. Berlin Heidelberg: Springer-Verlag, 2009. ISBN: 978-3-642-01099-6. DOI: 10.1007/978-3-642-01100-9. URL: <https://www.springer.com/gp/book/9783642010996> (visited on 05/30/2020).
- [91] Usman A. Syed et al. “From Roussettus aegyptiacus (bat) landing to robotic landing: Regulation of CG-CP distance using a nonlinear closed-loop feedback”. In: *2017 IEEE International Conference on Robotics and Automation (ICRA)*. May 2017, pp. 3560–3567. DOI: 10.1109/ICRA.2017.7989408.

BIBLIOGRAPHY

- [92] Shantanu Thakar et al. “A Survey of Wheeled Mobile Manipulation: A Decision-Making Perspective”. In: *Journal of Mechanisms and Robotics* 15.2 (Apr. 2023), p. 020801. DOI: 10.1115/1.4054611.
- [93] R.M. Voyles and A.C. Larson. “TerminatorBot: a novel robot with dual-use mechanism for locomotion and manipulation”. In: *IEEE/ASME Transactions on Mechatronics* 10.1 (Feb. 2005), pp. 17–25. DOI: 10.1109/TMECH.2004.842245.
- [94] ZhiFeng Wang et al. “A unified dynamic model for locomotion and manipulation of a snake-like robot based on differential geometry”. In: *Science China Information Sciences* 54.2 (Feb. 2011), pp. 318–333. DOI: 10.1007/s11432-010-4161-z.
- [95] P. Wiriyacharoensunthorn and S. Laowattana. “Analysis and design of a multi-link mobile robot (Serpentine)”. In: *2002 IEEE International Conference on Industrial Technology, 2002. IEEE ICIT '02*. Vol. 2. Dec. 2002, 694–699 vol.2. DOI: 10.1109/ICIT.2002.1189249.
- [96] Alon Wolf et al. “Design and control of a mobile hyper-redundant urban search and rescue robot”. In: *Advanced Robotics* 19.3 (Jan. 2005), pp. 221–248. DOI: 10.1163/1568553053583652.
- [97] *XL-GEN Manipulator - Robot for Research* — Robotnik®. en-US. URL: <https://robotnik.eu/products/mobile-manipulators/xl-gen/> (visited on 03/29/2024).
- [98] M Yamakita, Takeshi Yamada, and Kenta Tanaka. “Control of Snake Like Robot for Locomotion and Manipulation”. In: ().
- [99] M. Yim. “New locomotion gaits”. In: *Proceedings of the 1994 IEEE International Conference on Robotics and Automation*. May 1994, 2508–2514 vol.3. DOI: 10.1109/ROBOT.1994.351134.
- [100] Zhengxue Zhou et al. “Learning-based object detection and localization for a mobile robot manipulator in SME production”. In: *Robotics and Computer-Integrated Manufacturing* 73 (Feb. 2022), p. 102229. DOI: 10.1016/j.rcim.2021.102229.